RSC Advances

ROYAL SOCIETY OF CHEMISTRY

www.rsc.org/advances

Colour graphic	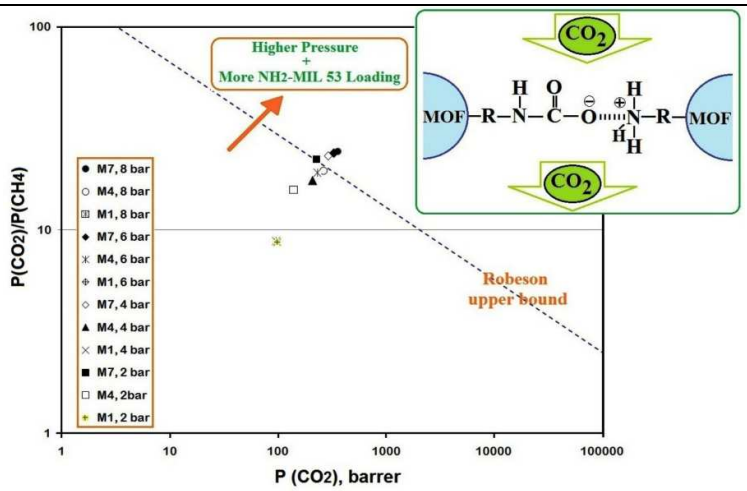
Text	PMP and NH_2-MIL53 were used for fabrication of a high permeable mixed matrix membrane with same trend between permeability and selectivity.

High Permeable Poly (4- methyl-1-pentyne)/NH_2-MIL 53 (Al) Mixed Matrix Membrane for CO_2/CH_4 Separation

Reza Abedini*, Mohammadreza Omidkhah*, Fatereh Dorosti

Faculty of Chemical Engineering, Tarbiat Modares University, P.O. Box 14115-143, Tehran, Iran

Abstract

Poly (4-methyl-1-pentyne) (PMP) as a polymer matrix together with synthesized NH_2-MIL 53 metal organic frame work (MOF) as a filler were used to fabricate a mixed matrix membrane (MMM). Various characterization methods as well as series of CO_2/CH_4 gas separation test (i.e. pure and mixed gas test) were conducted in order to determine the effect of NH_2-MIL 53 on properties of the prepared MMMs and their gas transport characteristics. Results of TGA and DMA showed that both degradation temperature (T_d) and glass transition temperature (T_g) increased by increasing NH_2-MIL 53 loading. SEM images also demonstrated that uniform dispersion of NH_2-MIL 53 particles in PMP matrix was achieved with no noticeable voids in the polymer-filler interfaces. It was also found that, incorporation of NH_2-MIL 53 in PMP results in increase of gases permeability (especially for CO_2) and higher CO_2/CH_4 selectivity. In contrast with the increment of CO_2 solubility due to presence of MOF in polymer matrix, the solubility of CH_4 decreases. Although the CO_2 solubility was improved with addition of NH_2-MIL 53, its diffusivity remained almost constant with no significant changes. Lastly, it was observed that increasing the MOF loading along with higher feed pressure provide a condition to overcome the Robeson upper bound.

Keywords: poly (4-methyl-1-pentyne), NH_2-MIL 53, mixed matrix membrane, metal organic frame work, CO_2/CH_4 separation

* Correspondence author: Tel.: +98 21 82883334; fax: +98 21 82883334
E-mails: r.abedini@modares.ac.ir (R. Abedini), omidkhahmodares.ac.ir (M. Omidkhah)

1. Introduction

Gas separation by means of membrane technology has increasingly gained interest, mainly because of the lower required energy, higher flexibility, working at low temperature and compact system structure.[1-3] Among the various types of polymers, the polymeric membranes have been widely used in membrane fabrication for gas separation processes mainly due to ease of fabrication and lower operating cost. Because of low chemical and thermal stability, and no acceptable selectivity of some polymeric membranes, fabrication of mixed matrix membranes (MMMs) was developed. Fabricated MMMs are based on the polymers and incorporation of different fillers such as metal oxides and carbon nano-tubes (CNTs), and also some porous materials such as zeolites, so that there is a potential to overcome the Robeson trade-off.[4] However, the impact of novel materials such as metal organic frameworks (MOFs) on the performance of MMMs has not comprehensively studied.[5] MOFs are specific categories of materials which are composed of metal ions as connectors and organic bridging ligands as linkers.[5] Creating the non-selective voids at the filler-polymer interface caused that recent studies have turned to the usage of fillers with higher affinity to polymer matrix. MOFs with broad functionalized ligands interact with polymer chain properly leading to prevention of non-selective voids in MOF and polymer interface.[6] Moreover, MOFs with high pore volume and specific cavities are able to absorb and separate particular gases which results in higher selectivity.[7] Impact of different MOFs on performance of MMMs has been investigated in various studies.[8-12]

The inclusion of amines in MOFs for the superior separation of CO_2 from different gases has been examined. The effects of these functionalized MOFs on the separation performance and polymer-filler compatibility of mixed matrix membranes have been investigated.

Seoane et al. studied the effects of NH_2-MIL 53 (Al) and NH_2-MIL 101 (Al) in sulfur-containing copolyimide mixed matrix membranes for gas separation process. 6FDA:DSDA/4MPD:4,40-SDA 1:1 (polymer P1) and 6FDA/4MPD:4,40-SDA 1:1 (polymer P2) were used for based

polymer matrix. The gas separation properties of MMMs evaluated through permeation of H_2, CH_4 and CO_2. The loading of NH_2-MIL53 in MMMs were 10 and 15 wt.% whereas 5 and 10 wt.% for NH_2-MIL 101. Using 10 wt.% of NH_2-MIL 101 in P1 caused that the permeability of H_2, CH_4 and CO_2 improved to 114, 1.7 and 71 Barrer respectively and the performance of MMMs was closeness to the Robeson upper bound for H_2/CH_4 and CO_2/CH_4.[13]

Impacts of NH_2-MIL 53 incorporation with polyimide were reported by Chen et al. NH_2-MIL 53 was added up to 36 wt.% to the polyimide. The permeability of CO_2 increased significantly by increasing MOF loading but remained unchanged for CH_4 in part. Like permeability, increasing of MOF loading led to the ideal selectivity (P_{CO_2} / P_{CH_4}) and consequently the separation factor (α CO_2:CH_4 = 50:50) was improved. The separation performance of MMM was decreased by 36 wt.% loading of MOF which could be due to the lower compatibility of NH_2-MIL 53 at higher loading and formation of non-selective voids in polymer-filler interfaces.[14]

Ghaffari Nik et al. investigated the effects of NH_2-UiO-66 (Zr-ABDC) and NH_2-MOF-199 as filler in polyimide MMMs. Both MOFs added to the polymer matrix with 25 wt.% loading. For the case of NH_2-UiO-66, presence of MOF in MMM resulted in permeability decline for both CO_2 and CH_4, while the ideal selectivity of CO_2/CH_4 increased. The results for NH_2-UIO-66 showed that the presence of "–NH_2" functional groups lead to creating rigidified chain at the polymer/filler interface, so that permeability reduced while selectivity improved. Unlike NH_2-UiO-66, incorporation of NH_2-MOF-199 with polyimide improved permeability of both gases (especially for CO_2) together with CO_2/CH_4 ideal selectivity.[15]

Chen et al. reported the effects of NH_2-MIL 53 with the loading of 8, 15 and 25 wt.% on gas separation characteristics of co-polyimide. Through addition of MOF, the permeability of MMMs enhanced compared to neat co-polyimide. They also showed that increasing the drying temperature of membrane after casting process resulted in better gas permeability together with higher selectivity.[16]

Impact of NH_2-MIL 53 particles on performance of PSF membrane was investigated by Valero et al. Results from Young's modulus and contact angle measurement suggested well dispersion of filler in polymer matrix. The optimum H_2/CH_4 separation factor of 67.34 with hydrogen permeability of 19.5 Barrer was achieved at 8 wt.% loading of NH_2-MIL 53.[17]

Incorporation of NH_2-MIL 53 in of Matrimid®5218 membrane improved the CO_2/CH_4 separation performance of MMM. At 15 wt.% loading of NH_2-MIL 53, CO_2/CH_4 selectivity increased up to 36.4. Although, the best selectivity obtained at 15 wt.% incorporated of NH_2-MIL 53, the permeability of CO_2 decreased from 10.4 Barrer at 8 wt.% loading to 9.2 Barrer at 15 wt.% loading of NH_2-MIL 53.[18]

Rodenas et al. investigated the performance of Matrimid®5218/NH_2-MIL 53 based MMM. NH_2-MIL 53 incorporated to Matrimid with 8, 15 and 25 wt.%. Increasing of NH_2-MIL 53 loading resulted in CO_2 permeability improvement from 7.3 Barrer to 14.6 Barrer at 8 and 25 wt.% loading of MOF respectively. Unlike permeability improvement, CO_2/CH_4 selectivity decreased from 38.3 to 34.8 at temperature of 308 K and pressure of 3 bar.[19]

Among different types of MOFs, MIL 53 has great tendency for selective CO_2 adsorption compared to other gases. It was found that isotherm of CH_4 and CO_2 differ significantly due to isotypical porous trephthaliates MIL 53. The molecular structure of MIL 53 with chemical formula of $[M(OH)(O_2C–C_6H_4–CO_2)$, $(M = Al^{3+}, Cr^{+3}, Fe^{3+})]$ comprise from infinite chains which share $M_4(OH)_2$ octahedra, interconnected with the dicarboxylate groups.[20]

Applications of glassy polymers which have high free volume (i.e., resulted from unoccupied space between molecules) have acquired considerable interests. These polymers such as PTMSP,[21,22] PTMGP [23,24] and PMP [25,26] are relatively more permeable to condensable large gases.

Poly (4- methyl-1- pentyne) (PMP) which is known as TPX, is a member of polyolefin group. PMP with low density, good chemical resistance, high thermal stability and especially high gases permeability is a promising nominee as a high permeable membrane.[27]

Therefore PMP is one of the alternative materials for fabrication of gas permeable membrane, in which the gas transport properties could be improved by embedding different kinds of filler in the polymer matrix that can surpass the Robeson upper bound.

The aim of this study is fabrication of MMM with appropriate filler and high free volume polymer. Thus, NH_2-MIL 53 (Al) with high affinity to CO_2 adsorption and high permeable PMP were selected as filler and based polymer respectively. The CO_2 and CH_4 adsorption-desorption test was conducted to evaluate adsorption properties of NH_2-MIL 53 (Al). Different MMMs were fabricated by adding MOF to the polymer from 0 to 30 wt. %. MOF and the prepared membranes were characterized by X-ray diffraction (XRD), FT-IR spectrum, thermal gravimetric analysis (TGA), dynamic mechanical analysis (DMA) scanning electron microscopy (SEM) and N_2 adsorption. Lastly, performance of pure PMP and MMMs were analyzed by constant volume gas permeation test and the results were compared with Robeson upper bound.

2. Materials and Methods

2.1. Materials

A PMP (Sigma Aldrich) with medium molecular weight was used for polymeric matrix of membrane. CCl_4 supplied by Merck was also used to prepare the casting solution. N, N-dimethylformamide or DMF (Merck), 2-amino terephthalic acid (NH_2-H_2BDC, Sigma Aldrich with purity of 99%), aluminium nitrate nonahydrate ($Al(NO_3)_3.9H_2O$, Sigma Aldrich with purity of 99%) and deionized water were employed for synthesis of amine functionalized MIL 53. MIL 53 (Al) from Sigma Aldrich without any preparing process was used to determine the exact effect of $–NH_2$ functional group on synthesized NH_2-MIL 53 (Al).

2.2. Synthesis of amine functionalized MIL-53

The synthesis of NH_2-MIL 53 (Al) was carried out according to the method proposed by Ahnfeldt et al.[28] First, 3.1 g of aluminium nitrate nonahydrate was dissolved in 1.5 g of 2-aminotereohthalic acid through Teflon-lined stainless steel autoclave. Once the solution was homogenised, 22.8 mL of deionized water was added to the solution. Thereafter, the prepared

mixture was heated at the temperature of 150 ºC and for a period of 5 h. Then the product was washed with acetone and thereafter collected by a centrifuge set at the speed of 6000 rpm for 10 min. To remove the incorporated NH_2-H_2BDC, the synthesized NH_2-MIL 53 washed with DMF twice, under 150 ºC for 48 h. Finally, the produced powder was dried in a vacuum oven at temperature of 150 ºC for 48 h.

2.3. Membrane preparation

PMP/MIL 53 (Al) flat sheet membranes were prepared via solution casting method by applying priming technique. First, NH_2-MIL 53 (Al) with pre-specified weight percent (wt. %) were mixed with CCl_4 under stirring for 6 hours. To ensure homogenous dispersion of MOFs in solvent, the mixture was sonicated for 10 min. Then PMP (5 wt. % by weight of solution) was added to the mixture (NH_2-MIL 53 + CCl_4) and dissolved in the solvent by 24 hours stirring. The solution was remained in the vacuumed oven with ambient temperature for six hours in order to remove any bubble which created during stirring process. Final mixture with admissible viscosity was casted on glass plate. For slow evaporation of solvent and to avoid of any defect in membrane formation, a small thin glassy dish was put over the casted film to allow 24 hours for solvent evaporation. To ensure that solvent was evaporated completely, formatted membrane was placed in a vacuumed oven with temperature of 50ºC for 12 hours. At the end, the membrane was simply separated from glass plate. The concentration of NH_2-MIL 53 (Al) in the casting solution varied from 0 to 30 wt. %. Table 1 presents the composition of each casting solution.

Table 1.

2.4. Characterization

X-ray diffraction (XRD) was conducted at room temperature using X'Pert MPD (Philips) diffractometer with the cupper as an anode and graphite as a cathode. The wave length of X-ray, its voltage and current were 1.54056 Å, 40 kV and 30 mA, respectively. The data were collected from $2\theta = 2 – 40^{o}$ with the scanning rate of 0.02 ^{o}/s.

Fourier transform infrared spectroscopy (FTIR) was performed using a PerkinElmer- 0.03.06. FTIR spectrometer. Spectra were recorded with an average of 50 scans in the wavenumber range of 4000–450 cm^{-1}, and with a resolution of 5 cm^{-1}.

The thermal degradation of polymer and the actual amount of NH_2-MIL 53 in polymer matrix were analysed by means of thermal gravimetric analyzer (TGA-50, Shimadzu). 20 mg of sample was loaded in a pretarred platinum pan which was pre-heated to 120 °C in order to remove moisture. When the sample was cooled down, it was reheated from temperature of 20 to 800 °C with a rate of 10 °C/min.

Dynamic mechanical analysis (DMA) was carried out to examine the glass transition of MMMs and their mechanical properties. The temperature was increased from ambient to 90 ºC with a rate of 5 ºC/min. Young's modulus of the membranes was also determined at various temperatures in the range of 25 – 200 ºC with 5 ºC/min heating rate and an amplitude of 75 µm. Tensile strength and elongation at break were also calculated at temperature of 25 ºC and action force up to 20 N.

Diffraction light scattering (DLS) analysis was utilized to determine the size of NH_2-MIL 53. In order to investigate the membrane structure and the quality of dispersion of NH_2-MIL 53 in polymer matrix, scanning electron microscopy (SEM) was performed using CamScan SEM model MV2300 microscope. The membranes were snapped under liquid nitrogen to give a generally unfailing and clean cut. The membranes were then sputter-coated with thin film of gold and mounted on brass plates with double-sided adhesive tape in a lateral position.

Nitrogen adsorption/desorption analysis (Belsorp mini II, BelJapan) was carried out to determine the textural characteristic of MOFs. The data were collected at temperature of 77 K and in the range of relative pressure (P/P_o) between 0.02 and 1.0. In order to calculate the transparent properties of MMMs, CO_2 and CH_4 adsorption isotherms were conducted on MIL 53 and NH_2-MIL 53. For each test, 0.5 g of particles was placed in a container at 303 K. The adsorption data was collected at pressures in the range of 0-10 bar and analysed by Langmuir Eq. as follow:

$$\frac{p}{q} = \frac{p}{q_m} + \frac{1}{b \times q_m} \quad (1)$$

Where p is adsorption pressure (kPa) and q is the amount of adsorbed gas in term of mmol/g. A regression technique was used to calculate q_m and b for each gas. In addition, Henry's law constant can be calculated by multiplying q_m and $b\,(K_H = q_m \times b)$.

2.5. Pure gas permeation

Pure CH_4 and CO_2 permeabilities were determined by means of constant volume system and calculated using the following equation:

$$P = \frac{273.15 \times 10^{10} VL}{760AT\left[(P_o \times 76)/14.7\right]}\left(\frac{dP}{dt}\right) \quad (2)$$

Where P is the gas permeability of membrane in Barrer (1 Barrer = 10^{-10} cm^3 (STP)-cm/cm^2.s.cmHg), V is the constant volume vessel (cm^3), L is the membrane thickness (cm), A is the membrane surface area (cm^2), T is the experiment temperature, P_o is the feed pressure (Psia) and (dP/dt) is the slope of pressure versus time.

The multiplication of solubility and diffusivity of each gas, gives the related permeability of the gas as presented as follows:

$$P = S \times D \quad (3)$$

The ideal selectivity is defined as the permeability ratio of two types of gas as it is given:

$$\alpha_{A/B} = \frac{P_A}{P_B} = \left(\frac{S_A}{S_B}\right) \times \left(\frac{D_A}{D_B}\right) \quad (4)$$

Where P_A and P_B are permeability of gas A and gas B respectively. (S_A/S_B) is solubility selectivity and (D_A/D_B) is diffusivity selectivity.

To calculate the diffusivity coefficient of each gas in membrane, the modified time lag method for mixed matrix membranes was used. Paul and Kemp proposed this method to represent the relationship between diffusivity (D) and time-lag (θ) in MMMs as:[28]

$$D = \frac{L^2}{6\theta}\left[1 + \left(\frac{V_d}{V_p}\right) K f(y)\right] \quad (5)$$

$$f(y) = \frac{6}{y^3}\left[\frac{1}{2}y^2 + y - (1+y)\ln(1+y)\right] \quad (6)$$

Where L is the membrane thickness (cm), θ is the time lag (s), V_d is the volume fraction of filler (in this case is MIL 53) and V_p is the volume fraction of polymeric phase $(V_d = 1 - V_p)$. K is constant and calculated from Langmuir adsorption parameters:

$$K = q_m b / K_H \quad (7)$$

Where K_H is Henry's law coefficient and $y = bp$ where b is Langmuir parameter and p is feed or upstream pressure.[29]

The main advantage of modified time lag method compared to time lag one (were $D = L^2 / 6\theta$) is that this method considers the effect of filler phase on gas diffusion in MMMs. It is worthwhile to mention that $L^2 / 6\theta$ can be derivate from Eq. 5 for the case of neat membrane. In neat membrane, V_d (the volume fraction of filler) equals to zero and Eq. 5 gives time lag method equation.

2.6. Mixed gas permeation

A binary mixture of CO_2 and CH_4 which containing 10 % of CO_2 was used as a feed gas in mixed gas test and permeability measurement of each gas conducted at 30 ºC and 2 bar using the following equation:

$$P_{CH_4} = \frac{273.15 \times 10^{10}(1 - y_{CO_2})VL}{760AT\left[(1 - x_{CO_2})(P_o \times 76)/14.7\right]}\left(\frac{dP}{dt}\right) \quad (8)$$

$$P_{CO_2} = \frac{273.15 \times 10^{10} y_{CO_2} VL}{760AT\left[(x_{CO_2}(P_o \times 76)/14.7\right]}\left(\frac{dP}{dt}\right) \quad (9)$$

Where P_{CH_4} and P_{CO_2} are he permeability of CH_4 and CO_2 respectively in Barrer, V is the constant volume vessel (cm^3), L is the membrane thickness (cm), A is the membrane surface area (cm^2), T is the experiment temperature, P_o is the feed pressure (Psia) and (dP/dt) is the slope of pressure versus time.

The gas mixture selectivity was calculated by the following equation:

$$\alpha_{A/B} = \frac{y_A / y_B}{x_A / x_B} \quad (10)$$

Where x and y are the mole fractions in the feed gas and permeate, respectively. A gas chromatography instrument (GC-model ACME 6100 Young Lin Instrument Co., Korea) with a thermal conductivity detector (TCD) and a Q capillary column was used for permeate analysis. The carrier gas was Helium.

3. Results and Discussions

3.1. Characterization of NH_2-MIL 53 and prepared MMMs

3.1.1. X- ray diffraction

Fig. 1 shows the XRD patterns of MIL 53 and NH_2-MIL 53. The corresponding peak of NH_2-MIL 53 depends on the visitor molecules were located in pores due to the breathing character.[13] The peak 10.5º corresponds to trapped unreacted 2-amino terephthalic acid.[13] Comparison between XRD results of MIL 53 and NH_2-MIL 53 indicated that the peak near 2θ = 12º can be related to $–NH_2$ group whereas similar to reported by Chen et al.[14] It seems that $–NH_2$ functional group in the MIL 53 structure affects the XRD spectrum, and subsequently on the crystal structure of the MOF. The XRD patterns of PMP, and MMM containing 15 wt.% of NH_2-MIL 53 also were illustrated in Fig. 1. The higher intensity peaks of 9.1º and 9.7º in MMM pattern obviously correspond to NH_2-MIL 53. Furthermore, the peaks of 9.1º and 15.8º belong to the lp and np configurations, respectively.[16] As Fig. 1 shows, for the MMM with 15 wt.% of NH_2-MIL 53, the lp structure is dominant in the membrane matrix.

Fig. 1.

3.1.2. Fourier transform infrared (FTIR) spectroscopy

FT-IR used for considering the interaction between polymer chains and fillers. FT-IR is one of the common methods for characterization of chemical bond in each phase and the bond created between chains and NH_2-MIL 53. Fig. 2 illustrated the FT-IR spectrums of MIL 53, NH_2-MIL 53, PMP, and MMMs containing 15 wt.% of NH_2-MIL 53. For MIL 53 and NH_2-MIL 53 the three characteristic peaks of carboxylate groups which are coordinated to Al, exist in spectra (1604 cm^{-1}, 1573 cm^{-1} and 1732 cm^{-1}). These peaks are related to asymmetric CO_2 stretching mode of carboxylic groups. The bands at 3656 and 3497/3385 cm^{-1} and the broad signals between 3000 and 2500 cm^{-1} are due to the bridging OH and the -NH_2 group, and the aminoterephthalic acid in the pores. For functionalized MIL 53, the two sharp bands at 3418 cm^{-1} and 3483 cm^{-1} show the –NH_2 group.[30] The free acid C=O bond (1687 cm^{-1}) in the pores of MOF is replaced by the C=O bond of the DMF molecules (1670 cm^{-1}). There are only two peaks at 3450 and 3617 cm^{-1} in the MIL 53 curve at wavenumbers above 2000 cm^{-1}. These peaks correspond to the O–H bond and can be seen in other MMMs FTIR results too (at 3627 $cm^{-1}$for 5 wt.% MOF loading and at 3622 $cm^{-1}$for 15 wt.% MOF loading).

Two monomeric residue units in Poly (4-methyl-1-pentyne) are repeated in every structural unit. Since there are methyl group in the side chain which the asymmetric stretching modes of –CH_3 are assigned to 2973 and 2954 cm^{-1}. CH_3 symmetric stretching modes corresponded to very strong bands at 2888 and 2869 cm^{-1}.[31]

The poly methylene chain with –CH_2–CH–$(CH_3)_2$ as the side group is attached to every second carbon atom. The bands at 2971, 2949, 2928 and 2887 cm^{-1} all corresponded to the CH asymmetric stretching in CH_3 and the bands of 2864 cm^{-1} shows the CH symmetric stretching. Moreover the C-C stretching is specified via bands of 1102, 1063, 1054 and 996 cm^{-1}. The C-C bonds in plane bending were shown by the bands with frequency of 618, 540, 528 and 449 cm^{-1}.[31]

The MMM with 15 wt.% loading of NH_2-MIL 53 has the similar peaks compare to the PMP neat membrane. There exists some shifting which are mainly due to the interaction between NH_2-MIL 53 and polymer chains. The peaks at 3421 and 3488 cm^{-1} indicated the presence of $–NH_2$ group and the amino terephthalic acid in the pores. The bands at 1021 cm^{-1} in MIL 53, NH_2-MIL 53 and M4 corresponded to C – O – Al bond.

Fig. 2.

3.1.3. Thermal and mechanical analysis

Fig. 3 depicts the weight reduction of MIL 53, NH_2-MIL 53, neat polymeric membrane, and MMMs as a change of temperature. It is shown that TGA curve of each sample has three discrete parts. The degradation temperature of NH_2-MIL 53 was lower than that of MIL 53 together with more weight loss in the first section of TGA curve. The more weight loss can be due to the $–NH_2$ group of NH_2-MIL 53 which decomposes at lower temperatures.[32] In addition, the C–H bond in MIL 53 is stronger than the C–N bond in NH_2-MIL 53 and decomposes at higher temperatures, leading to the higher thermal stability of MIL 53. The thermal degradation of the neat PMP initiates at temperature of 320 ºC which is related to the polymer degradation. T_d of MMMs increased up to 350 ºC because of high thermal stability of NH_2-MIL 53 and existence of complimentary interaction between NH_2-MIL 53 and PMP chains.[33] The strong covalent bond between NH_2-MIL 53 and polymer may enhance the rigidity of chains and increase the required energy for breaking down the PMP chains.[34]

The amount of NH_2-MIL 53 as a filler in polymer matrix can be accurately measured via the remained weight loss in TGA curves. Except for NH_2-MIL 53 and because of its $–NH_2$ group, the first and third section of TGA curves for each sample, shows no significant weight loss which is mainly due to the weight have been occupied with remained solvent.

Fig. 3.

Fig. 4 shows the tanδ curve and modulus (E') for pure PMP and selected MMMs as a change in temperature. The peaks of tanδ curve (i.e., $d\tan\delta / dT$ equal to zero), show the glass transition

temperature of prepared membranes. For instance, it is seen that a peak at 43 ºC represents the T_g of pure PMP which is the same as the previously reported T_g for PMP. [35,36] The T_g of MMMs increased with increase of NH_2-MIL 53 loading. The chain movement restriction as a result of the interaction between polymer chains and MOFs leads to the T_g increment.[37,38] As shown, the storage modulus of pure PMP was 1370 MPa at 0 ºC. Storage modulus of PMP deceases by increasing temperature and reaches 301 MPa at 80 ºC. The MMMs show higher storage modulus over the entire temperature. The presence of NH_2-MIL 53 strengthens and reinforces the PMP chains which subsequently results in increase of the modulus storage for MMMs

Fig. 4.

Table 2 presents the mechanical properties of filled PMP membranes with 10, 20 and 30 wt.% loading of NH_2-MIL 53 loading. Tensile strength and elongation at break decreased by increasing the NH_2-MIL 53 loading. During the membrane formation, NH_2-MIL 53 may agglomerate. These agglomerated decrease tensile strength and elongation at break with two ways. First, chain disruptions can occur and the second, the concentration of stress is higher around of agglomerated MOFs.[9] A significant enhancement of Young's modulus might be due to well dispersion of fillers in polymer matrix and acceptable interaction between polymer chains and NH_2-MIL 53.[10]

Table 2.

3.1.4. Morphological study of membranes

With the knowledge of the initial size of NH_2-MIL 53 particles, the impact of agglomeration of MOFs in polymer matrix can be investigated in more details. Fig. 5a and b depict the DLS and SEM image analyses of MIL 53. As Fig. 5a shows, most of the MIL 53 particles have a size of around 100 nm in terms of intensity and volume. In addition, the SEM image of particles (Fig. 5b) clearly confirms the results obtained by DLS analysis.

Fig. 5.

Quality of NH_2-MIL 53 dispersion within the polymer matrix was investigated by means of scanning electron microscopy analysis. Fig. 6 shows the SEM photograph of top layer of prepared membranes. Some particles agglomeration can be seen on the top layer of MMMs with 10 and 30 wt. % of NH_2-MIL 53, however the dispersion of particles was appropriately uniform. Fig. 6d shows the interface of polymer and particle with higher magnification.

Fig. 7 also depicts the cross sectional photograph of the prepared membranes. For the MMM with 30 wt.% loading of particles, NH_2-MIL 53 dispersed uniformly in the membrane. Fig. 7d and 7e illustrate the NH_2-MIL 53 and its interface with polymer matrix with higher magnification. As it is shown, there are almost no noticeable voids at the polymer/filler interface. Furthermore, cross sectional images confirm that at higher loading of NH_2-MIL 53 (i.e., 30 wt.%), some particle agglomeration formed in the polymer matrix. Fig. 7f and g reveals the cross sectional image of M1 and M4 with lower magnification. As Fig. 7g and g shown, prepared membranes have a thickness of 60 to 70 nm.

Fig. 6.

Fig. 7.

3.1.5. Gas adsorption characteristics

Fig. 8 portrays the N_2 sorption performed at 77 K. The results obtained from BET analysis were also presented in Table 3. According to the results plotted in Fig. 8, the amount of adsorbed N_2 by NH_2-MIL 53 was significantly less than that by MIL 53 which confirms the BET results. Moreover, the specific surface area, mesopore surface area, micropore, mesopore, and total volume of NH_2-MIL 53 were lower than those of MIL 53. Pore size distribution can also be inferred from the adsorption isotherm assuming a given model of adsorption. BJH (Barrett-Joyner-Halenda) method used for calculating pore size distributions is based on a model of the adsorbent as a collection of cylindrical pores. A detail procedure of this method was reported by Barrett et al.[39]

Since the $–NH_2$ group was connected to $–H_2BDC$ ligands, the pore diameter of functionalized MIL 53 reduced to 0.83 nm compared to 0.91 nm of MIL 53. The percentage reduction of all textural characteristics for MIL 53 and NH_2-MIL 53 is given in Table 3.

Fig. 8.

Table 3.

To investigate the adsorption properties of NH_2-MIL 53 compared to those of MIL 53, the CO_2 and CH_4 adsorption isotherms were conducted at different pressures up to 10 bar and temperature of 303 K and the results for each MOF are shown in Fig. 9. CO_2 uptake of MIL 53 and NH_2-MIL 53 increased with increased adsorption pressure. The strong interaction between positive charges on the unsaturated open Aluminium and quadro-polarity of CO_2 results in significant amount of CO_2 adsorption.[29] CO_2 adsorption isotherm indicated that MIL 53 has greater potential to adsorb CO_2 more than NH_2-MIL 53. This behaviour confirms the BET results and reported previously for other similar amine-functionalized MOF.[14,15] At pressures lower than 6.3 bar, more amount of CO_2 adsorbed by NH_2-MIL 53 compared to MIL 53 mainly due to presence of $–NH_2$ group. This behaviour of amine-functionalized MOF was reported for other similar adsorbent.[40-42] For CH_4, the amount of CH_4 uptake increased because of increase in adsorption pressure.

Unlike CO_2, the amount of adsorbed CH_4 was imperceptible at pressure lower than 2 bar which is in agreement with the results reported by Couck et al.[43] This difference between adsorbed CO_2 and CH_4 is as a result of the presence of $–NH_2$ groups located on the aromatic linker of terephthalic acid which reduces the polar adsorption sites.[44]

The overall CO_2/CH_4 sorption selectivities for MIL 53 and NH_2-MIL 53 were 2.60 and 2.56, respectively, where similar to the reported by Stavitiski et al.[45] At pressures lower than 6.3 bar, the selectivity of NH_2-MIL 53 was more than that of MIL 53.

The adsorption characteristics of MIL 53 and NH_2-MIL 53 were analysed based on the Langmuir equation. The values of q_m and b of Langmuir determined via regression analysis of the data

shown in Fig. 9 and are listed in Table 4. It was found that the q_m for MIL 53 which has higher surface area and pore volume is higher than that for NH_2-MIL 53 with lower surface area and pore volume. Henry's constant, which reflect the adsorption strength of gases was presented in Table 4 for both CO_2 and CH_4. K_H of gases for MIL 53 adsorbent was higher than NH_2-MIL 53 which confirms the superior adsorption capability of MIL 53 compared to amine functionalized one. Although Henry's constant used for adsorption analysis at lower pressure, but according to Langmuir model which emphasis on layer adsorption of gases, K_H can be calculated through multiplication of q_m and b.

Table 4.

Fig. 9.

3.2. Pure gas permeation properties

3.2.1. Permeability and selectivity

Table 5 presents the permeability and selectivity of all prepared membranes in this study. The permeability of gases was determined by taking an average from three replicates permeation at temperature of 30 ºC and pressure of 2 bar. Permeability of CO_2 and CO_2/CH_4 ideal selectivity increased with increasing NH_2-MIL 53 loading in MMMs. Moreover, for all membranes, it was observed that the permeability of CO_2 was significantly higher than that of CH_4. In addition to higher condensability and lower kinetic diameter of CO_2 which results in higher CO_2 permeability, presence of functional $–NH_2$ group in MIL 53 improves the permeability of CO_2 during the process. There are two main reasons lead to the enhancement of CO_2 permeability through addition of NH_2-MIL 53 to PMP. First, NH_2-MIL 53 increases the free volume of PMP and provides a condition so that higher amount of CO_2 is condensed in the polymer matrix. The second, NH_2-MIL53 is more prone to adsorb CO_2 rather than CH_4 which could be mainly due to the $–NH_2$ functionalized group.

Effect of NH_2-MIL 53 loading on free volume of polymer was determined through calculation of fractional free volume (FFV) as follows:

$$FFV = \frac{V - V_0}{V} \quad (11)$$

Where V is specific volume (cm^3/g), V_0 is the volume occupied by PMP chains. V_0 can be calculated as $V_0 = 1.3V_W$ in which V_W is the vas der waals volume estimated by the group contribution method.[15] The FFV of PMP and MMMs are reported in Table 6.

Table 5.

Table 6.

The selectivity of CO_2/CH_4 increased from 11.85 with 5 wt.% of MOF loading to 22.36 when the MOF loading increased to 30 wt.%. The increase in the selectivity of CO_2/CH_4 depends on three main mechanisms:

i) The high free volume of PMP caused that gases pass through the membrane with dominant solubility. In glassy polymer also, presence of different kinds of particles (in this case MOF) can disrupt chains and increase the free volume of polymer. By this means, between CO_2 and CH_4, CO_2 with higher condensability permeates more than CH_4.[46]

ii) The R-NH_2 group in NH_2-MIL 53 reacts reversibly with CO_2 molecules and forms the carbamate.[47] According to Fig. 10, this reaction enhances the permeability of CO_2 compared to CH_4 and results in the increment of CO_2/CH_4 selectivity.

iii) Functional –NH_2 group significantly increases the affinity between polymer chains and MOF because of formatted hydrogen bond between –NH_2 of MIL 53 and polymer. Although this bond rigidifies the polymer chain and consequently reduces the probability of non-selective voids formation, thereby it noticeably improves the selectivity of CO_2/CH_4.

Fig. 10.

Normalized permeability of CO_2 and CH_4 together with normalized CO_2/CH_4 ideal selectivity are shown in Fig.11. This figure depicts the variation of both gas permeability and the CO_2/CH_4 selectivity more obvious. In contrast with non-modified MOF, the modified one has a smaller

pore size which is mainly attributed to additional $–NH_2$ group. This can be considered as the main reason for CH_4 permeability reduction. It is noteworthy to mention that the similar trend was seen for CO_2 permeability and CO_2/CH_4 selectivity.

Fig. 11.

3.2.2. Diffusivity and solubility coefficient in MMM

Diffusion and dissolution of gases are the principal parameters affecting their permeability. In order to characterize gas transport properties of MMMs, diffusivity and solubility coefficients of CO_2 and CH_4 were calculated. Diffusivity and solubility coefficients of CO_2 and CH_4 in pure PMP and PMP/NH_2-MIL 53 mixed matrix membranes together with their diffusivity and solubility selectivities are presented in Table 7.

Table 7.

The diffusivity coefficient was calculated using the modified time-lag method. The diffusivity of CO_2 and CH_4 almost remained constant by increasing NH_2-MIL 53 loading. The diffusivity is influenced by free volume of MMMs, diffusion through MOF pore, and quality of surface compatibility between polymer chains and functional MOF.[48] Each of aforementioned parameters has a different impact on diffusivity. Increasing the free volume of membrane due to the addition of NH_2-MIL 53 facilitates and enhances the diffusion of gases. Despite free volume, the pore size of NH_2-MIL 53 is smaller than that of MIL 53 which inhibits the passage of gases. A proper compatibility between polymer chains and MOF decreases the probability of non-selective void formation. The effect of this compatibility is obvious at higher NH_2-MIL 53 loading which resulted the diffusivity of both CO_2 and CH_4 to be decreased.

Solubility coefficient of CO_2 increased from 17.24 to 37.43 barrer by increasing the NH_2-MIL 53 loading from 5 to 30 wt.% in MMM, respectively. High affinity of NH_2-MIL 53 to adsorb CO_2 and higher condensability led to such significant increase in solubility coefficient of CO_2. In contrast with CO_2, lack of noticeable interaction between $–NH_2$ group and CH_4 along with lower condensability of CH_4 caused that the solubility of CH_4 did not effectively improved.

As it is presented in Table 7, all diffusivity selectivity (D_{CO_2} / D_{CH_4}) values for MMM are lower than those for pure PMP. On the other hand, solubility selectivity (S_{CO_2} / S_{CH_4}) increased by increasing NH_2-MIL 53 loading. Compared to neat PMP, all MMMs have higher solubility selectivity because of impressive CO_2 sorption by amine functionalized MIL 53. It is important to notify that the NH_2-MIL 53 fillers in MMM separate gases based on preferential adsorption of CO_2, not size sieving. Consequently this phenomenon may leads to the more solubility selectivity of MMM compared with pure PMP.

Fig. 12 illustrates the variation of solubility, diffusivity and ideal selectivity as a change of NH_2-MIL 53 loading in membrane. It is seen that solubility selectivity has a significant responsibility in ideal selectivity increment.

Fig. 12.

3.2.3. Effect of feed pressure on the performance of PMP/NH_2-MIL 53 MMM

Table 8 tabulates the effect of feed pressure on permeability and selectivity of both CO_2 and CH_4. For PMP, increasing the feed pressure leads to a slight decrease in CO_2 and CH_4 permeability. According to the dual sorption model (DSM) in glassy polymer, increasing the feed pressure results in permeability decline. Increasing the penetrant concentration in polymer matrix as a result of increasing the feed pressure enhances the polymer plasticization, especially for strong condensable gases.[46] On the other hand, high induced pressure on membrane leads to the compactness of polymer chains, thereby fractional free volume (FFV) along with penetrant diffusion coefficient reduces. Unlike neat PMP, MMMs showed opposite behaviour at higher feed pressures. Based on CO_2 adsorption isotherm by NH_2-MIL 53 the amount of adsorbed CO_2 increases significantly as the adsorption pressure increases. Alternatively, CO_2 molecules have tendency to pass through membrane via condensation and sorption processes. Increasing the feed pressure causes that the concentration of condensable CO_2 in polymer to be increased and the plasticization effect of the soluble CO_2 to be enhanced. Thus the solubility of condensable CO_2 in polymer matrix increased by increasing the feed pressure. Since CH_4 diffuses in polymer

through free volume, increasing in feed pressure provides an appropriate condition for CH_4 to further diffuse and permeate.[48,49]

As table 8 shows, the permeability of CO_2 and CH_4 increased from98.74 and 11.32 barrer to 358.18 and 14.70 barrer (for M7 at 8 bar) respectively.

Table 8.

Fig. 13 depicts the effect of feed pressure on ideal selectivity of MMMs. The selectivity of neat PMP (M1) increased slightly from 8.72 to 8.81. In addition, it was found that the ideal selectivity of MMMs (M4 and M7) is increased. The CO_2/CH_4 selectivity of MMM with 15 wt.% loading of NH_2-MIL 53 increased from 15.72 at pressure of 2 bar to 19.53 at 8 bar. For 30 wt.% loading of NH_2-MIL 53 (M7), the CO_2/CH_4 selectivity increased from 22.36 at 2 bar to 24.35 at the pressure of 8 bar. This effect can be attributed to a more favourable condensability as well as more sorption of CO_2 by NH_2-MIL 53. Since there is a lower condensability along with less sorption for CH_4, CO_2 permeability increased significantly at higher pressures compared to the permeability of CH_4 and higher selectivity was achieved.[50] Cohen and Turnball proposed a correlation to determine the diffusion coefficient using free volume of polymer as it is given:[51]

$$D_i = \alpha \exp\left(\frac{-\gamma v_i}{V_{FV}}\right) \tag{12}$$

Where α is a factor that depends on temperature, V_{FV} is average free volume of polymer and γv_A is penetrant size.

According to Eq. 12, increasing the free volume of polymer results in reduction of the impact of diffusivity selectivity (D_A / D_B) in ideal selectivity. Therefore, solubility selectivity is a key factor and playing an important role in overall selectivity. It means that solubility is a dominant factor due to the increasing in free volume of PMP. In this case, presence of NH_2-MIL 53 leads to the higher free volume of membrane. Moreover, sorption of CO_2 by MOF increased as pressure increased, and this higher amount of sorption along with higher free volume leads to the enhancement of CO_2/CH_4 selectivity.

Fig. 13.

3.3. Mixed gas permeation

The mixed gas permeation property of MMMs was investigated through the gas mixtures of CO_2/CH_4 ratios of 10:90 v/v. After passing of gas mixtures through the membrane, the impermeable flow was removed and thereafter, the gas composition of permeable gas flow was determined by utilizing the GC. The results of the permeability and selectivity of gas mixture at pressure of 2 bar and temperature of 30 ºC are presented in Table 9.

Comparing the results presented in Table 9 with those of the pure gas permeability data (i.e., Table 6) reveals that in all of the MMMs, the permeability values of CO_2 as well as the selectivity of CO_2/CH_4 are lower than those of pure gases. The reduction of CO_2 permeability and the subsequent decrease in the selectivity values are due to the presence of CH_4 in the mixture. In fact, the co-presence of other CH_4 with the CO_2 prevents the pass of CO2 through the membrane. The presence of the CH_4 in mixture reduces the CO_2 permeability mainly due to the two following reasons:

i) The presence of CH_4 in the mixture prevents further absorption of CO_2 by MOF particles.

ii) The presence of CH_4 in the mixture inside the membrane, more specifically inside the free volume of the membrane, prevents the more condensation of CO_2 which can reduce the CO_2 solubility.

The results also showed that the presence of CH_4 reduces the selectivity of the mixture so that, the maximum selectivity of PMP/NH_2-MIL 53 MMM decreased from 22.36 (in pure permeation) to 17.00 in the CO_2/CH_4 mixture.

Table 10 presents the impact of feed pressure on the performance of MMMs containing MOF particles in the separation of gas mixture. The trend of changes in permeability and selectivity were almost the same as pure gas permeability and ideal selectivity of CO_2/CH_4 selectivity, respectively. It was also found that the permeability of CO_2 and the real selectivity were lower

than corresponding values of pure permeability and ideal selectivity. For CO_2 case, the permeability of 339.48 Barrer and selectivity of 22.87 were the most efficient performance of PMP/NH_2-MIL 53 which was observed at pressure of 8 bar.

Table 10

The results presented in Table 10 indicate that although the interaction between the gases in the gas mixture prevents the pass of CO_2 through membrane, the MMMs show an appropriate performance to separate the CO_2 mixtures.

3.4. Permeability and selectivity at higher loading of NH_2-MIL 53

According to Fig. 14 adding NH_2-MIL 53 at higher loading values results in the reduction of the permeability of CO_2 and CH_4. It was observed that the permeability of CO_2 and CH_4 was decreased at 40 wt.% loading of NH_2-MIL 53 to 216.71 and 9.87 Barrer compared to MMM with containing 35 wt.% of MIL 53 (i.e. CO_2 permeability and CO_2/CH_4 selectivity of 224.47 barrer and 9.87 respectively). In addition, the selectivity values at 30, 35, and 40 wt.% loadings of NH_2-MIL 53 were found to be almost unchanged. The main reason for permeability reduction of CO_2 at higher loading of NH_2-MIL 53 is attributed to the considerable decrease in its diffusion coefficient as a result of the presence of high amount of particles in the polymer matrix. High amount of NH_2-MIL 53 particles in the polymer matrix of membrane rigidifies polymer chain extremely and elongates the diffusion path of CO_2, thereby reduces the diffusion coefficient of the CO_2. In addition, the high percentage of NH_2-MIL 53 particles improves CO_2 solubility coefficient together with solubility selectivity. Therefore, it was concluded that the 30 wt.% NH_2-MIL 53 is the optimum loading in the membrane matrix and provides the most appropriate performance compared to other MMMs.

Fig. 14.

3. 5. Separation performance of MMMs

Table 11 summarizes the results of CO_2/CO_4 separation using MMM in which MOF was used as filler. As it is shown, the permeability and selectivity of each MMM are strong functions of

MOF structure, polymer properties, process parameters, and its affinity to CO_2. Comparison of the results of this study with those of previously published work showed that PMP/NH_2-MIL 53 MMMs have significantly higher permeability along with satisfactory range of selectivity.

The performance of all synthesized membranes for CO_2/CH_4 separation is presented in Figs. 15 and 16. It is shown that higher pressures provide the condition to approach the Robeson bound. Figs. 15 and 16 confirm that incorporation of NH_2-MIL 53 in PMP along with higher upstream pressure enhance the selectivity of CO_2/CH_4. Furthermore, the trend of selectivity versus CO_2 permeability shows the behaviour against the Robeson curve trade off. The high free volume of polymer, more condensability of CO_2, high affinity of NH_2-MIL 53 to adsorb CO_2, and higher upstream pressure are the main parameters providing the condition to overcome the Robeson upper bound. Generally, membranes with high permeability and acceptable selectivity are definitely more attractive to industry. Significant increase of CO_2 permeability (i.e., from 98.74 barrer at 2 bar and no loading of MOF to 358.18 barrer at 8 bar and 30 wt.% loading of MOF in pure permeation) and noticeable improvement of selectivity (i.e., from 8.72 to 24.4) were obtained via using NH_2-MIL 53 for the prepared MMM. Thus, it is believed that amine-functional groups (e.g., NH_2-MIL 53) are appropriate fillers for MMMs. Fig. 16 also confirms that against the reduction in CO_2 permeability and CO_2/CH_4 selectivity in mixed gas test (i.e. 339.5 Barrer and 22.8), the performance of MMM at 8 bar and 30 wt.% loading of MOF surpasses Robeson upper bound.

Table 8.

Fig. 15 .

Fig. 16 .

4. Conclusions

In this study, synthesized NH_2-MIL 53 was incorporated in PMP to prepare MMMs with extensive gas permeation properties. TGA and DMA analyses revealed that the thermal and mechanical properties such as degradation temperature, tensile strength and Young's modulus of

MMMs improved by increasing the MOF loading. It was found that presence of NH_2-MIL 53 in PMP matrix results in noticeable improvement of CO_2 permeability. In addition, increasing the free volume of MMMs together with high affinity of NH_2-MIL 53 to adsorb CO_2 led to the higher CO_2 permeability and solubility coefficient. Unlike CO_2, enhancing the diffusivity coefficient of CH_4 increased CH_4 permeability slightly. CO_2/CH_4 selectivity in MMMs increased from 8.72 to 22.36 at pressure of 2 bar by increasing the MOF loading with dominant solubility selectivity. Moreover, it was obtained that increasing the feed pressure improves the permeability and selectivity of MMMs. A similar trend in permeability and CO_2/CH_4 selectivity was a remarkable property of PMP/NH_2-MIL 53 MMMs. This character together with higher feed pressure ranging from 2 to 8 bar provided a condition for MMMs to overcome the Robeson upper bound. Finally the permeability and selectivity of MMMs (i.e., M7) obtained in this study were significantly improved compared with those of pure PMP. Generally, it seems that $-NH_2$ functionalized MIL 53 is an appropriate filler to incorporate with PMP based on MMM for CO_2/CH_4 separation.

Symbols

p	adsorption pressure (kPa)
q	adsorbed gas (mmol/g)
q_m	maximum adsorbed gas (mmol/g)
b	Langmuir eq. parameter
K_H	Henry's law constant
P	Permeability (Barrer)
V	constant volume vessel (cm^3)
L	membrane thickness (cm)
A	membrane surface area (cm^2)
P_o	feed pressure (Psia)
T	Temperature (K)
S	gas solubility (cm^3(STP) cm^{-3} $cmHg^{-1}$)
D	gas diffusivity (cm^2/s)
$\alpha_{A/B}$	selectivity
θ	time-lag (s)
V_d	volume fraction of filler
V_p	volume fraction of polymeric phase
X	mole fractions in the feed
y	mole fractions in the permeate
FFV	fractional free volume
V_0	volume occupied by PMP chains
V_W	vas der waals volume
V_{FV}	average free volume of polymer
γv_A	penetrant size

References

1. M. Zamani Pedram, M.R. Omidkhah and A. Ebadi Amooghin, Synthesis and characterization of diethanolamine-impregnated cross-linked polyvinylalcohol/glutaraldehyde membranes for CO_2/CH_4 separation, *J. Ind. Eng. Chem.*, 2014, 20, 74-82.

2. L. Shao and T.S. Chung, In situ fabrication of cross-linked PEO/silica reverse-selective membranes for hydrogen purification, *Int. J. Hydrogen Energy*, 2009, 34, 6492 – 6504.

3. R. Abedini, S. M. Mousavi and R. Aminzadeh, A novel cellulose acetate (CA) membrane using TiO_2 nanoparticles: Preparation, characterization and permeation study, *Desalination*, 2011, 277, 40–45.

4. I. Erucar, G. Yilmaz and S. Keskin, Recent advances in metal–organic framework-based mixed matrix membranes, *Chem. Asian J.*, 2012, 41, 14003–14027.

5. L. Lin, L. Zhang, C. Zhang, M. Dong, C. Liu, A. Wang, Y. Chu, Y. Zhang and Z. Cao, Membrane adsorber with metal organic frameworks for sulphur removal, *RSC Adv.,* 2013, **3**, 9889-9896.

6. J. Caro, Are MOF membranes better in gas separation than those made of zeolites? *Curr. Opin. Chem. Eng.*, 2011, 1, 77–83.

7. X. Duan, Y. He, Y. Cui, Y. Yang, R. Krishna, B. Chen and Guodong Qian, Highly selective separation of small hydrocarbons and carbon dioxide in a metal–organic framework with open copper (II) coordination sites, *RSC Adv.*, 2014, **4**, 23058-23063.

8. Y. Zhang, I. H. Musselman, J. P. Ferraris and K. J. Balkus, Gas permeability properties of Matrimid® membranes containing the metal-organic framework Cu–BPY–HFS, *J. Membr. Sci.*, 2008, 313, 170–181.

9. F. Dorosti, M. Omidkhah and R. Abedini, Fabrication and characterization of Matrimid/MIL-53 mixed-matrix membranes for CO_2/CH_4 separations, *Chem. Eng. Res. Des.*, 2014, doi: 10.1016/j.cherd.2014.02.018

10. S. Basu, A. Cano-Odena and I.F.J. Vankelecom, MOF-containing mixed-matrix membranes for CO_2/CH_4 and CO_2/N_2 binary gas mixture separations, *Sep. Purif. Technol.*, 2011, 81, 31–40.

11. R. Abedini, M. Omidkhah and F. Dorosti, CO_2/CH_4 separation by using poly methyl pentene/MIL 53 particles mixed matrix membrane, *Iranian J. Polym. Sci. Technol.,* 2014, **27**, 18-27.

12. E.V. Perez, K. J. Balkus, J. P. Ferraris and I. H. Musselman, Mixed-matrix membranes containing MOF-5 for gas separations, *J. Membr. Sci.*, 2009, 328, 165–173.

13. B. Seoane, C. Téllez, J. Coronas and C. Staudt, NH_2-MIL-53(Al) and NH_2-MIL-101(Al) in sulfur-containing copolyimide mixed matrix membranes for gas separation, *Sep. Purif. Technol.*, 2013, 111, 72‑81.

14. X. Y. Chen, H. Vinh-Thang, D. Rodrigue and S. Kaliaguine, Amine-functionalized MIL-53 metal−organic framework in polyimide mixed matrix membranes for CO_2/CH_4 Separation, *Ind. Eng. Chem. Res.*, 2012, 51, 6895−6906.

15. O. Ghaffari Nik, X. Y. Chen and S. Kaliaguine, Functionalized metal organic framework-polyimide mixed matrix membranes for CO_2/CH_4 separation, *J. Membr. Sci.*, 2012, (413‑ 414), 48‑61.

16. X. Y. Chen, H. Vinh-Thang , D. Rodrigue and Serge Kaliaguine, Optimization of continuous phase in amino-functionalized metal–organic framework (MIL-53) based co-polyimide mixed matrix membranes for CO_2/CH_4 separation**,** *RSC Adv.*, 2013, **3**, 24266-24279.

17. M. Valero, B. Zornoza, C. Téllez and J. Coronas, Mixed matrix membranes for gas separation by combination of silica MCM-41 and MOF NH_2-MIL-53(Al) in glassy polymers, *Micoropor. Mesopor. Mater.,* 2014, **192**, 23-24.

18. T. Rodenas, M. Dalen, P. Serra-Crespo, F. Kapteijn and J. Gascon, Mixed matrix membranes based on NH_2-functionalized MIL-type MOFs: Influence of structural and operational parameters on the CO_2/CH_4 separation performance, *Micoropor. Mesopor. Mater.,* 2014, **192**, 35-42.

19. T. Rodenas, M. Dalen, E. García-Pérez, P. Serra-Crespo, B. Zornoza, F. Kapteijn , and J. Gascon, Visualizing MOF Mixed Matrix Membranes at the Nanoscale: Towards Structure-Performance Relationships in CO_2/CH_4 Separation Over NH_2-MIL-53(Al)@PI, *Adv Funct. Mater.,* 2014, **24**, 249-256.

20. A. Boutin, F.X. Coudert, M.A. Springuel-Huet, A.V. Neimark, G. Fe´rey and A.H. Fuchs, The Behavior of Flexible MIL-53(Al) upon CH_4 and CO_2 Adsorption, *J. Phys. Chem. C*, 2010, 114, 22237–22244.

21. I. Pinnau, C. G. Casillas, A. Morisato and B. D. Freeman, Hydrocarbon/hydrogen mixed gas permeation in poly(1-trimethylsilyl-1-propyne) (PTMSP), poly(1-phenyl-1-propyne) (PPP), and PTMSP/PPP blends, *J. Polym. Sci., Part B: Polym. Phys.*, 1996, 34, 2613-2621.

22. S. Matteucci, A. Kusuma-Victor, D. Sanders, S. Swinea and B.D. Freeman, Gas transport in TiO_2 nanoparticle-filled poly(1-trimethylsilyl-1-propyne), *J. Membr. Sci.*, 2008, 307, 196-217.

23. V. Khotimskiy, M. Chirkova, E. Litvinova, M. Konrad, N. Lencerf, W. Yave, S. Shishatskiy and K.V. Peinemann, Poly(1-trimethylgermyl-1-propyne): synthesis, characterisation and transport properties of pure polymers and nanocomposites, *Desalination*, 2006, 199, 198-209.

24. A. Trusov, S. Legkov, L.J.P. Broeke, E. Goetheer, V. Khotimsky and A. Volkov, Gas/liquid membrane contactors based on disubstituted polyacetylene for CO_2 absorption liquid regeneration at high pressure and temperature. *J. Memb. Sci.*, 2011, 383, 241-249.

25. W. Yave, S. Shishatskiy, V. Abetz, S. Matson, E. Litvinova and V.Khotimskiy, A novel poly(4-methyl-2-pentyne)/TiO_2 hybrid nanocomposite membrane for natural gas conditioning: butane/methane separation, *Macromol. Chem. Phys.*, 2007, 208, 2412-2418.

26. T. C. Merkel, B. D. Freeman, R. J. Spontak, Z. He, I. Pinnau, P. Meakin and A. J. Hill, Sorption, transport, and structural evidence for enhanced free volume in poly (4-methyl-2-pentyne)/fumed silica nanocomposite membranes. *Chem. Mater.*, 2003,15, 109-118.

27. S. D. Wanjale and J. P. Jog, Poly (4-methyl-1-pentyne)/clay nanocomposites: effect of organically modified layered silicates, *Polym. Int.*, 2004, 53, 101–105.

28. T. Ahnfeldt, D. Gunzelmann, T. Loiseau, D. Hirsemann, J. Senker, G. Fe´rey and N. Stock, Synthesis and Modification of a Functionalized 3D Open-Framework Structure with MIL-53 Topology, *Inorg. Chem.*, 2009, 48, 3057-3064.

29. D.R. Paul and D.R. Kemp, The diffusion time lag in polymer membranes containing adsorptive fillers, *J. Poly. Sci. Poly. Symposia*, 1973, 41, 79–93.

30. H. Fan, H. Xia, C. Kong and L. Chen, Synthesis of thin amine-functionalized MIL-53 membrane with high hydrogen permeability, *Int. J. Hydrogen Energy*, 2013, 38, 10796-10802.

31. E.J. Samuel and S. Mohanb, FTIR and FT Raman spectra and analysis of poly(4-methyl-1-pentyne), *Spectrochim. Acta.*, 2004, 60, 19–24.

32. R. Abedini, M. Omidkhah and F. Dorosti, Hydrogen separation and purification with poly (4-methyl-1-pentyne)/MIL 53 mixed matrix membrane based on reverse selectivity, *Int. J. Hydrogen Energy*, 2014, 56, 7897-7909.

33. Y. Hu, L. Wu, J. Shen and M. Ye, Amino-functionalized multiple-walled carbon nanotubes-polyimide nanocomposite films fabricated by in situ polymerization, J. *Appl. Polym. Sci.*, 2008, 110, 701–705.

34. R. Abedini, S. M. Mousavi and R. Aminzadeh, Effect of sonochemical synthesized TiO_2 nanoparticles and coagulation bath temperature on morphology, thermal stability and pure water flux of asymmetric cellulose acetate nanocomposite membranes prepared via phase inversion method, *Chem. Ind. Chem. Eng. Q.*, 2012, 18, 385-398.

35. S. Bourrelly, P.L. Llewellyn, C. Serre, F. Millange, T. Loiseau and G. Férey, Different adsorption behaviors of methane and carbon dioxide in the isotypic nanoporous metal terephthalates MIL-53 and MIL-47, *J. Am. Chem. Soc.*, 2005, 127, 13519- 13521.

36. T. Tanigami, K. Yamaura, S. Matsuzawa and K. Miyasaka, Thermal expansion of crystal lattice of isotactic poly(4-methyl-1-pentyne), *Polym. J.*, 1986, 18, 35-40.

37. B. G. Ranby, K. S. Chan and H. Brumberger, Higher-order transitions in poly(4-methyl-1-pentyne) *J. Polym. Sci.*, 1962, 58, 545-552.

38. X. Y. Chen, H. Vinh-Thang, D. Rodrigue and S. Kaliaguine , Effect of macrovoids in nano-silica/polyimide mixed matrix membranes for high flux CO_2/CH_4 gas separation, *RSC Adv.*, 2014,**4**, 12235-12244.

39. E.P. Barrett, L.G. Joyner and P.P. Halenda, The determination of pore volume and area distributions in porous substances: Computations form nitrogen isotherms, *J. Am. Chem. Soc.,* 1951, 73, 373–380.

40. R.V. Siriwardane, M.S. Shen, E.P. Fisher and J.A. Poston, Adsorption of CO_2 on molecular sieves and activated carbon, *Energy Fuels*, 2001, 15, 279–284.

41. T.H. Bae, J.S. Lee, W. Qiu, W.J. Koros, C.W. Jones and S. Nair, A high-performance gas-separation membrane containing submicrometer-sized metal-organic framework crystals, Angew. *Chem. Int. Ed.*, 2010, 49, 9863–9866.

42. Q. Yang and C. Zhong, Molecular simulation of carbon dioxide/methane/hydrogen mixture adsorption in metal-organic frameworks, *J. Phys. Chem. B.*, 2006, 110, 17776–17783.

43. S. Couck, J. F. M. Denayer, G. V. Baron, T. Re´my, J. Gascon and F. Kapteijn, An amine-functionalized MIL-53 metal-organic framework with large separation power for CO_2 and CH_4, *J. Am. Chem. Soc.*, 2009, 131, 6326–6327.

44. F. Zhang, X. Zou, X. Gao, S. Fan, F. Sun, H. Ren and G. Zhu, Hydrogen selective NH_2-MIL-53(Al) MOF membranes with high permeability, *Adv. Funct. Mater.*, 2012, 22, 3583–3590.

45. E. Stavitski, E. A. Pidko, S. Couck, T. Remy, E. J. M. Hensen and B. M. Weckhuysen, J. Denayer, J. Gascon, F. Kapteijn, Complexity behind CO_2 capture on NH_2-MIL-53(Al), *Langmuir*, 2011, 27, 3970–3976.

46. F. Dorosti, M.R. Omidkhah, M.Z. Pedram and F. Moghadam, Fabrication and characterization of polysulfone/polyimide–zeolite mixed matrix membrane for gas separation, *Chem. Eng. J.*, 2011, 171, 1469– 1476.

47. M. Caplow, Kinetics of carbamate formation and breakdown, *J. Am. Chem. Soc.*, 1968, 90, 6795–6803.

48. F. Moghadam, M.R. Omidkhah, E. Vasheghani-Farahani, M.Z. Pedram and F. Dorosti, The effect of TiO_2 nanoparticles on gas transport properties of Matrimid5218-based mixed matrix membranes, *Sep. Purif. Technol.*, 2011, 77, 128-136.

49. T. C. Merkel, B. D. Freeman, R. J. Spontak, Z. He, I. Pinnau, P. Meakin and A. J. Hill, Ultrapermeable, reverse-selective nanocomposite membranes, *Science*, 2002, 296, 519-522.

50. J. Li, Y. Ma, M. C. McCarthy, J.Sculley, J.Yub, H.K. Jeong,, P. B. Balbuenab and H.C. Zhoua, Carbon dioxide capture-related gas adsorption and separation in metal-organic frameworks, *Coord. Chem. Rev.*, 2011, 255, 1791–1823.

51. M. H. Cohen and D. Turnbull, Molecular transport in liquids and glasses, *J. Chem. Phys.*, 1959, 31, 1164-1169.

52. B. Zornoza, B. Seoane, J. M. Zamaro, C. Téllez and J. Coronas, Combination of MOFs and zeolites for mixed-matrix membranes, *Chem. Phys. Chem.*, 2011, 12, 2781–2785.

53. K. Diaz, L. Garrido, M. Lopez-Gonzalez, L. F. del Castillo and E. Riande, CO_2 transport in polysulfone membranes containing zeolitic imidazolate frameworks as determined by permeation and PFG NMR techniques, *Macromolecules*, 2010, 43, 316–325.

Figure Captions

Fig. 1. XRD spectra of MIL 53, NH_2-MIL-53, neat PMP and PMP/NH_2-MIL 53 with 15 wt.% loading

Fig. 2. FTIR spectra of MIL 53, NH_2-MIL 53, PMP, PMP/15 wt. % NH_2-MIL53

Fig. 3. Thermal gravimetric analysis (TGA) curve of MIL 53, NH_2-MIL 53 and MMMs with loading of 10, 20 and 30 wt.% of MOF

Fig. 4. (a) tanδ curve, (b) Storage modulus versus temperature for PMP (M1), PMP/10 wt. % MOF (M3), PMP/20 wt. % MOF (M5) and PMP/30 wt. % MOF (M7)

Fig. 5. (a) DLS analysis of NH_2-MIL 53, (b) SEM image of NH_2-MIL 53 particles

Fig. 6. Top surface SEM image of (a) neat PMP, (b) PMP/10 wt. % MOF and (c) PMP/30 wt. % MOF, (d) NH_2-MIL 53 particle on the surface of membrane

Fig. 7. Cross sectional SEM image of (a) neat PMP, (b) PMP/10 wt. % MOF, (c) PMP/30 wt. % MOF, (d) quality of NH_2-MIL 53 and polymer chains interface, (e) polymer/particle interface at higher magnification, (f) cross sectional image of neat PMP with membrane thickness, (g) cross sectional image of MMM containing 20 wt.% of NH_2-MIL 53 with membrane thickness

Fig. 8. N_2 adsorption- desorption of MIL 53 and NH_2-MIL 53 at 77 K

Fig. 9. CO_2 and CH_4 adsorption isotherms of MIL 53 and NH_2-MIL 53 samples at 30 ºC

Fig. 10. Schematic view of reaction between CO_2 and R-NH_2 group to form carbomate formation where facilitated the CO_2 permeation

Fig. 11. Normalized permeabilities of CO_2 and CH_4 gases and CO_2/CH_4 ideal selectivities versus NH_2-MIL 53 loading

Fig. 12. Effect of NH_2-MIL 53 loading on solubility, diffusivity and CO_2/CH_4 ideal selectivities

Fig. 13. Effect of pressure on the selectivity of neat PMP (M1) and MMMs (M4 and M7)

Fig. 14. The effect of NH_2-MIL 53 loading on (a) permeability and CO_2/CH_4 selectivity, (b) solubility and CO_2/CH_4 solubility selectivity (c) diffusivity and CO_2/CH_4 diffusivity selectivity

Fig. 15. Performance of synthesized MMMs prepared with different weight fractions of NH_2-MIL 53 as well as pure PMP membrane in pure gas permeation compared to Robeson upper bound at 2, 4, 6 and 8 bar

Fig. 16. Performance of synthesized MMMs prepared with different weight fractions of NH_2-MIL 53 as well as pure PMP membrane in mixed gas permeation compared to Robeson upper bound at 2, 4, 6 and 8 bar

Table Captions

Table 1. Solution composition of pure and each MMMs membrane

Table 2. Mechanical properties of NH_2-MIL 53 filled PMP membranes at different loadings

Table 3. BET analysis of MIL 53 (Al) and NH_2-MIL 53 (Al)

Table 4. Langmuir parameters of MIL 53 and NH_2-MIL 53 for CO_2 and CH_4 adsorption at 303 K and 1-10 bar

Table 5. Averaged pure gas permeabilities (in Barrers), ideal selectivities of pure PMP and MMMs at 30 ºC and 2 bar

Table 6. Calculated FFV for neat PMP and MMMs

Table 7. Averaged pure gas diffusion and solubility coefficients for as-synthesized membranes

Table 8. Effect of pressure on pure CO_2 and CH_4 permeability in pure PMP and MMMs

Table 9. Averaged mixed gas permeabilities (in Barrers), real selectivities of pure PMP and MMMs at 30 ºC and 2 bar

Table 10. Effect of pressure on CO_2 permeability and real selectivity in pure PMP and MMMs for mixed gas permeation

Table 11. A comparison between CO_2/CH_4 separation data for selected MOFs based MMMs and this work

Table 1 Solution composition of pure and each MMMs membrane

Membrane Code	Polymer (5 wt. %)		Solvent (wt. %)
	PMP	NH_2- MIL 53 (Al)	CCl_4
M1	100	0	95
M2	95	5	95
M3	90	10	95
M4	85	15	95
M5	80	20	95
M6	75	25	95
M7	70	30	95

Table 2 Mechanical properties of NH_2-MIL 53 filled PMP membranes at different loadings

Membrane	Tensile strength (MPa)	Elongation at break (%)	Young modulus (GPa)
PMP	132 ± 2	116 ± 5	3.65 ± 0.2
PMP/10 wt. % MOF	120 ± 3	109 ± 2	3.89 ± 0.1
PMP/20 wt. % MOF	112 ± 2	101 ± 3	4.18 ± 0.1
PMP/30 wt. % MOF	107 ± 4	92 ± 3	4.34 ± 0.3

Table 3 BET analysis of MIL 53 (Al) and NH_2-MIL 53 (Al)

Sample	S_{BET} (m^2/g)	S_{meso} (m^2/g)	V_{micro} (cm^3/g)	V_{meso} (cm^3/g)	V_{total} (cm^3/g)	D_P (nm)
MIL 53 (Al)	1408	254	0.462	0.283	0.547	0.91
NH_2-MIL 53 (Al)	795	143	0.258	0.137	0.338	0.83
Reduction percentage	43.5	43.7	45.1	51.5	38.2	8.7

Table 4 Langmuir parameters of MIL 53 and NH_2-MIL 53 for CO_2 and CH_4 adsorption at 303 K and 1-10 bar

Sample	Gas	q_m (mmol/g)	$b\times10^3$ (kPa^{-1})	$K_H\times10^2$ (mmol/g kPa)
MIL 53 (Al)	CH_4	1.42	3.76	2.79
	CO_2	3.84	4.27	2.35
NH_2-MIL 53 (Al)	CH_4	1.36	3.81	2.57
	CO_2	3.75	4.49	2.16

Table 5 Averaged pure gas permeabilities (in Barrers), ideal selectivities of pure PMP and MMMs at 30 ºC and 2 bar

Membrane code	Permeability (barrer)		P_{CO_2} / P_{CH_4}
	CO_2	CH_4	
M1	98.74	11.32	8.72
M2	107.32	9.05	11.85
M3	118.74	9.43	12.59
M4	139.56	8.87	15.72
M5	164.78	8.92	18.46
M6	203.44	10.08	20.18
M7	226.37	10.12	22.36

Table 6 Calculated FFV for neat PMP and MMMs

Membrane code	M1	M3	M5	M7	M9
FFV	0.283	0.307	0.322	0.359	0.374

Table 7 Averaged pure gas diffusion and solubility coefficients for as-synthesized membranes

Membrane code	Diffusivity (10^{-7} cm^2/s)		Solubility ($10^{-3}cm^3$(STP) cm^{-3} $cmHg^{-1}$)		$\frac{D_{CO_2}}{D_{CH_4}}$	$\frac{S_{CO_2}}{S_{CH_4}}$
	CO_2	CH_4	CO_2	CH_4		
M1	61.37	16.67	16.10	6.82	3.82	2.47
M2	62.14	16.61	17.24	5.45	3.74	3.16
M3	63.29	17.15	18.76	5.58	3.69	3.42
M4	62.75	17.87	22.24	4.97	3.51	4.47
M5	61.53	16.76	26.78	5.17	3.57	5.17
M6	61.20	17.63	33.24	5.72	3.47	5.81
M7	60.47	15.84	37.43	6.38	3.81	5.86

Table 8 Effect of pressure on pure CO_2 and CH_4 permeability in pure PMP and MMMs

Feed pressure (bar)	Membrane code	MIL 53 loading (wt. %)	CO_2 permeability (barrer)	CH_4 permeability (barrer)
2	M1	0	98.74	11.32
	M4	15	139.56	8.87
	M7	30	226.37	10.12
4	M1	0	97.82	11.20
	M4	15	208.68	11.92
	M7	30	290.55	12.57
6	M1	0	97.05	11.13
	M4	15	231.63	12.11
	M7	30	328.48	13.75
8	M1	0	96.54	10.95
	M4	15	264.26	13.53
	M7	30	358.18	14.70

Table 9 Averaged mixed gas permeabilities (in Barrers), real selectivities of pure PMP and MMMs at 30 ºC and 2 bar

Membrane code	Permeability (barrer)		α_{CO_2/CH_4}
	CO_2	CH_4	
M1	83.35	10.95	8.05
M2	97.65	9.68	9.87
M3	112.39	10.02	10.04
M4	126.72	9.49	10.71
M5	150.69	9.57	12.10
M6	191.82	10.64	14.37
M7	210.21	10.58	17.00

Table 10 Effect of pressure on CO_2 permeability and real selectivity in pure PMP and MMMs for mixed gas permeation

Feed pressure (bar)	Membrane code	MIL 53 loading (wt. %)	CO_2 permeability (barrer)	α_{CO_2/CH_4}
2	M1	0	83.35	7.61
	M4	15	126.72	13.34
	M7	30	204.44	19.18
4	M1	0	81.18	7.74
	M4	15	189.75	14.88
	M7	30	272.18	19.88
6	M1	0	80.21	7.94
	M4	15	222.51	17.15
	M7	30	311.22	20.12
8	M1	0	80.10	8.12
	M4	15	244.61	18.24
	M7	30	339.48	22.87

Table 11. A comparison between CO_2/CH_4 separation data for selected MOFs based MMMs and this work

Polymer	MOF	Loading (wt. %)	Operating conditions		P_{CO_2}	P_{CH_4}	$\frac{P_{CO_2}}{P_{CH_4}}$	Ref.
			P	T				
Matrimid®	CU-BPY-HFS	10	2.7 bar	35 ºC	7.8	0.24	31.9	8
Matrimid®	CU-BPY-HFS	30	2.7 bar	35 ºC	10.4	0.38	27.5	8
Matrimid®	ZIF-8	30	5 bar	35 ºC	0.68[a]	0.021[a]	31.5	10
Matrimid®	MIL 53 IAl)	30	5 bar	35 ºC	0.71[a]	0.022[a]	32.0	10
Matrimid®	$Cu_3(BTC)_2$	30	5 bar	35 ºC	0.65[a]	0.019[a]	33.0	10
Copolyimide (P1)	NH_2-MIL 101	10	3 bar	35 ºC	70.9	1.7	41.6	13
Copolyimide (P2)	NH_2-MIL 101	10	3 bar	35 ºC	151.0	5.1	29.6	13
Copolyimide (P1)	NH_2-MIL 53	10	3 bar	35 ºC	56.9	1.6	35.8	13
Copolyimide (P2)	NH_2-MIL 53	10	3 bar	35 ºC	137.0	5.0	27.2	13
6FDA-ODA	NH_2-MIL 53	15	150 psi	30 ºC	14.3	0.27	52. 6	14
6FDA-ODA	NH_2-MIL 53	30	150 psi	30 ºC	16.2	0.23	70.43	14
6FDA-ODA	UiO-66	25	150 psi	35 ºC	40.4	1.10	44.1	15
6FDA-ODA	NH_2-UiO-66	25	150 psi	35 ºC	13.7	0.27	46.1	15
6FDA-ODA	MOF-199	25	150 psi	35 ºC	21.8	0.43	51.2	15
6FDA-ODA	NH_2-MOF-199	25	150 psi	35 ºC	26.6	0.45	59.6	15
PSF	ZIF-8	16	2 bar	30 ºC	12.1	0.61	19.8	52
PEES	ZIF-8	30	5 bar	35 ºC	50	2.40	20.8	53
PMP	NH_2-MIL 53	30	8 bar	30 ºC	358.2	14.7	24.4	This work
PMP	NH_2-MIL 53	30	8 bar	30 ºC	339.5[b]	14.9[b]	22.8	This work

[a)] Permeability calculated in terms of GPU
[b)] Mixed gas permeability

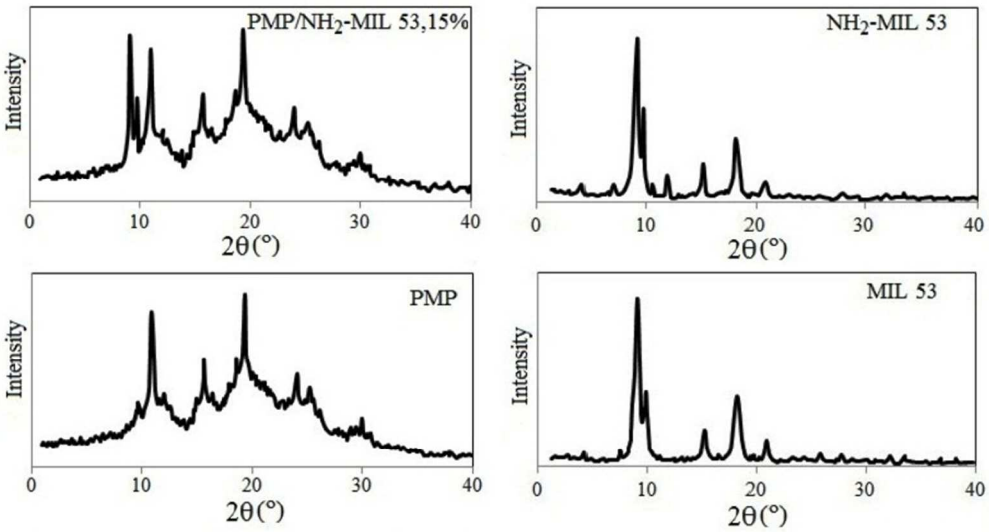

Fig. 1. XRD spectra of MIL 53, NH2-MIL-53, neat PMP and PMP/NH2-MIL 53 with 15 wt.% loading
242x131mm (96 x 96 DPI)

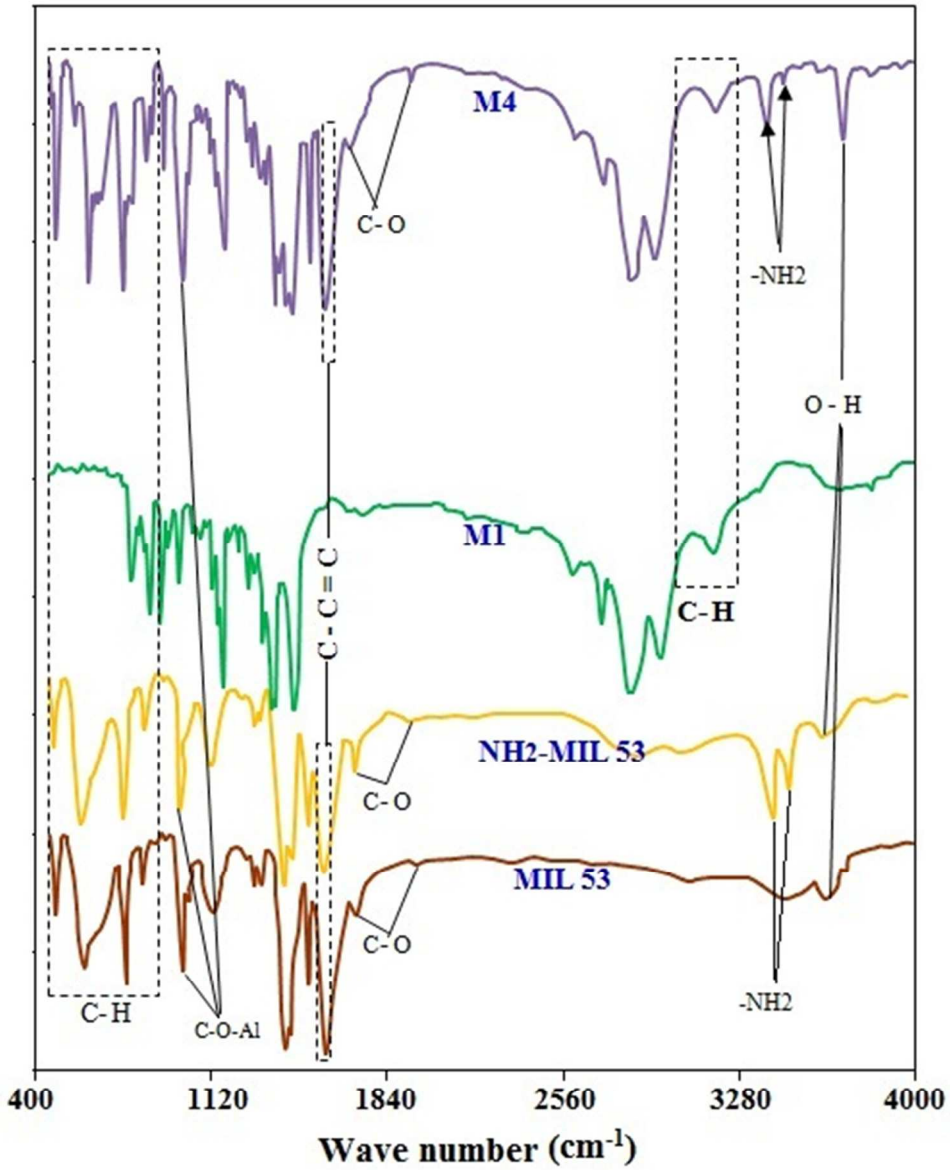

Fig. 2. FTIR spectra of MIL 53, NH2-MIL 53, PMP, PMP/15 wt. % NH2-MIL53
131x164mm (96 x 96 DPI)

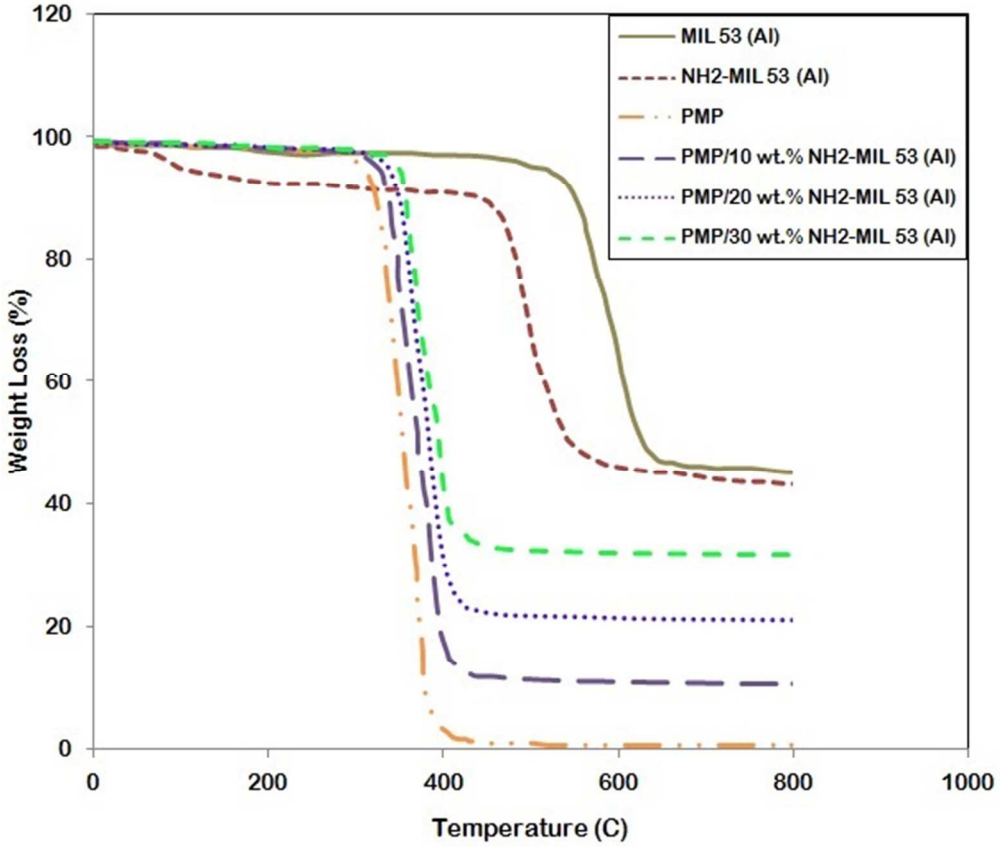

Fig. 3. Thermal gravimetric analysis (TGA) curve of MIL 53, NH2-MIL 53 and MMMs with loading of 10, 20 and 30 wt.% of MOF
160x138mm (96 x 96 DPI)

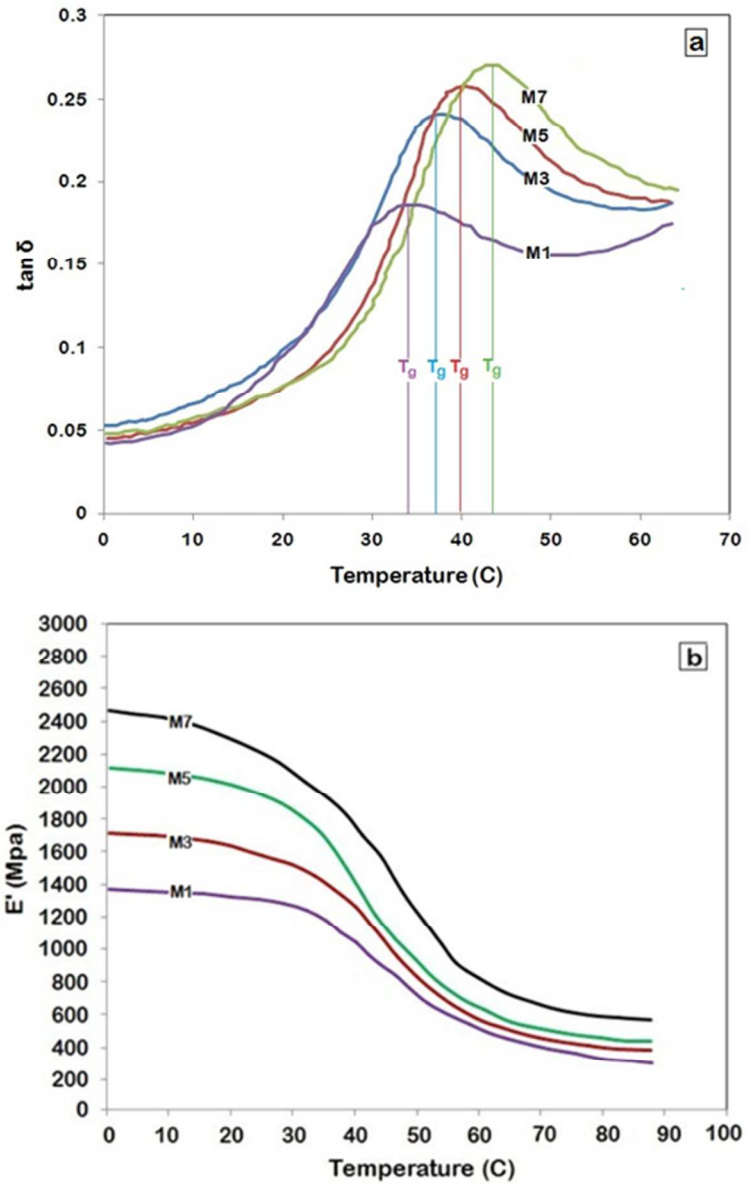

Fig. 4. (a) tanδ curve, (b) Storage modulus versus temperature for PMP (M1), PMP/10 wt. % MOF (M3), PMP/20 wt. % MOF (M5) and PMP/30 wt. % MOF (M7)
141x216mm (96 x 96 DPI)

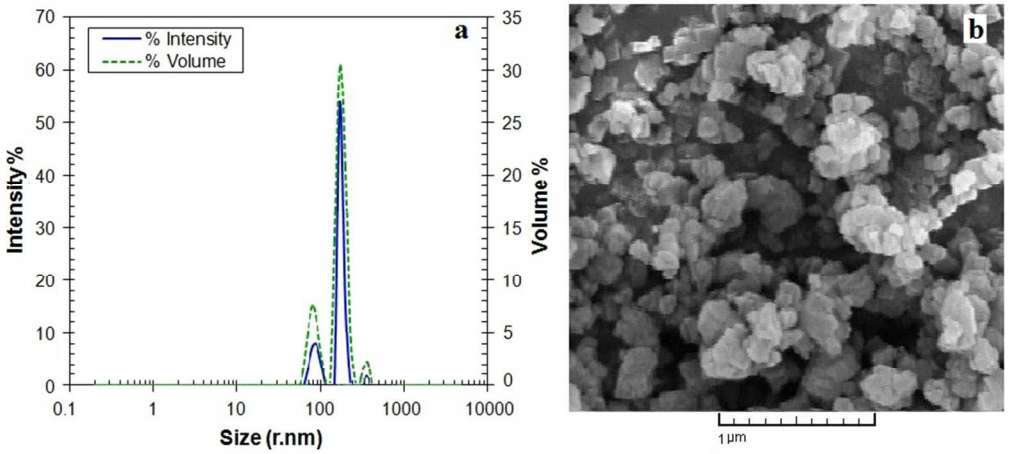

Fig. 5. (a) DLS analysis of NH2-MIL 53, (b) SEM image of NH2-MIL 53 particles
241x110mm (96 x 96 DPI)

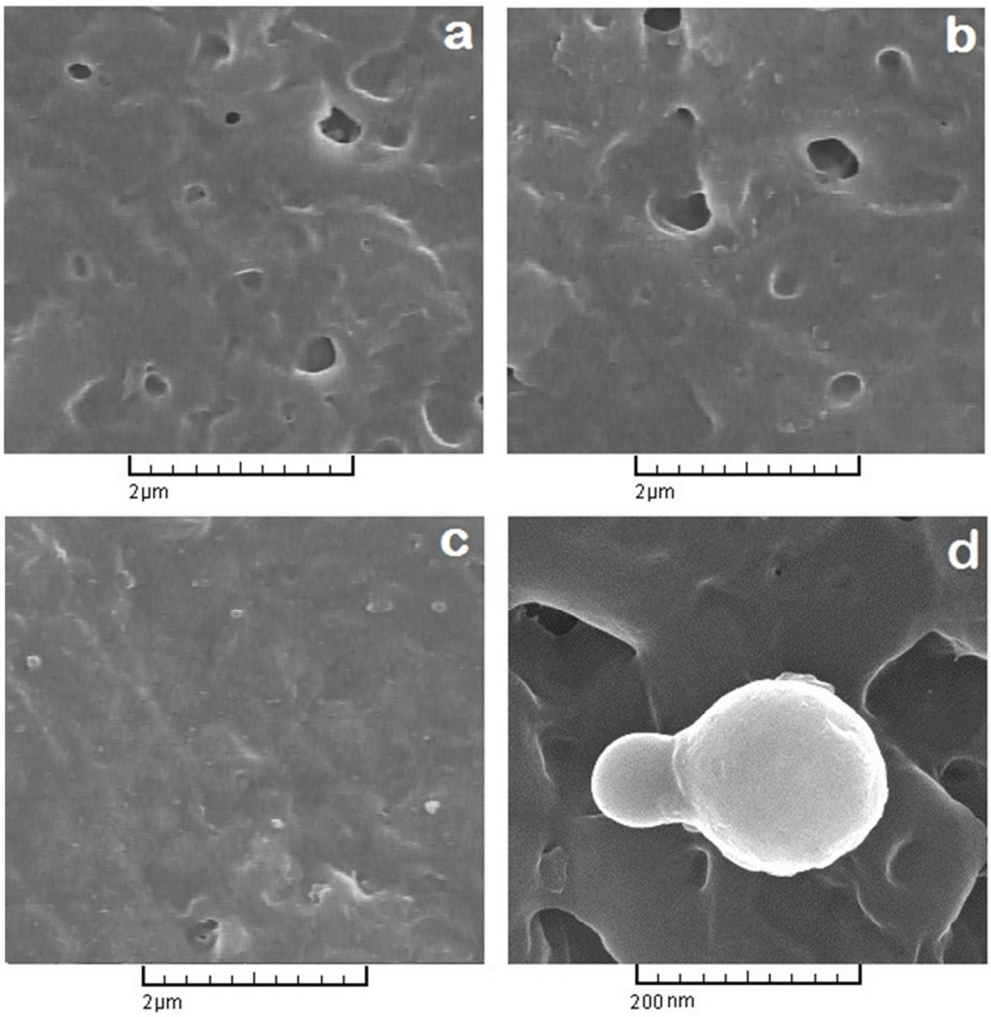

Fig. 6. Top surface SEM image of (a) neat PMP, (b) PMP/10 wt. % MOF and (c) PMP/30 wt. % MOF, (d) NH2-MIL 53 particle on the surface of membrane
257x267mm (96 x 96 DPI)

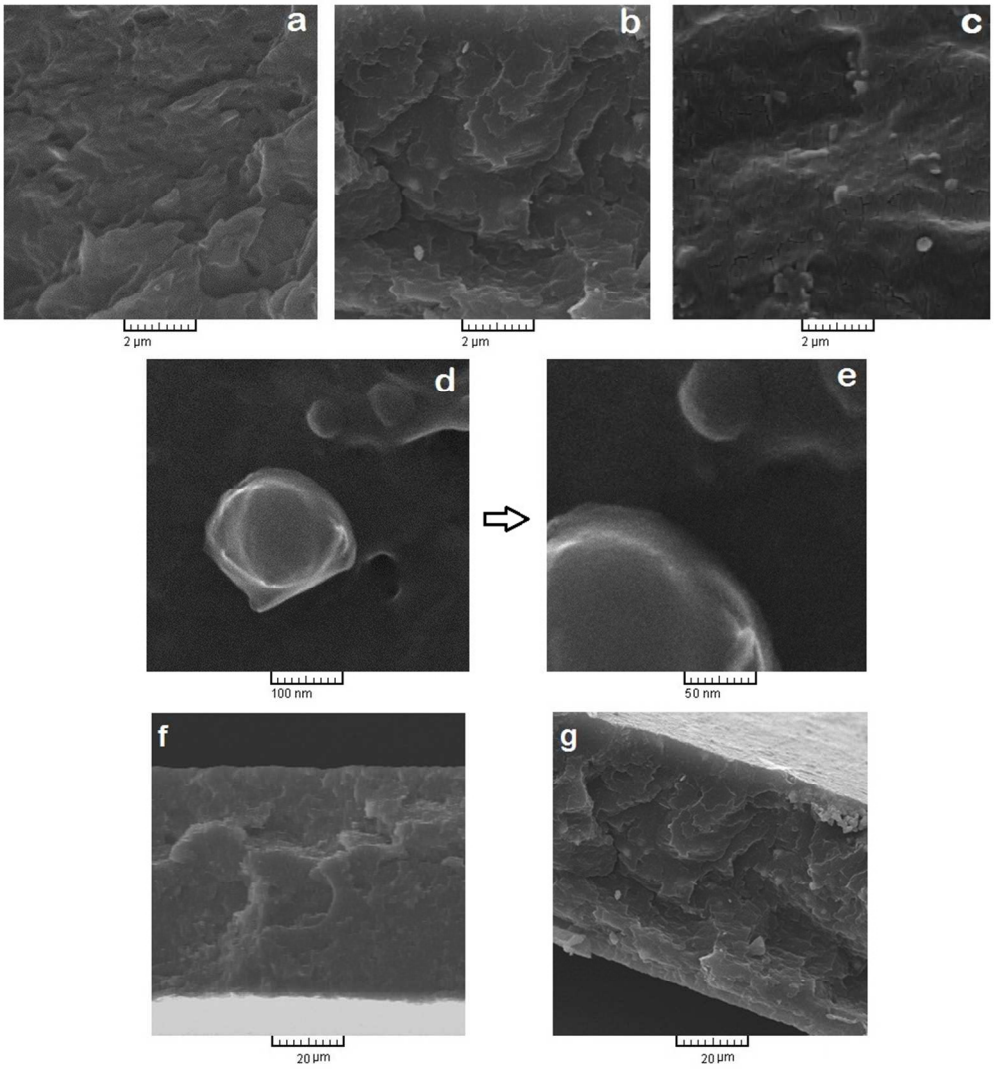

Fig. 7. Cross sectional SEM image of (a) neat PMP, (b) PMP/10 wt. % MOF, (c) PMP/30 wt. % MOF, (d) quality of NH2-MIL 53 and polymer chains interface, (e) polymer/particle interface at higher magnification, (f) cross sectional image of neat PMP with membrane thickness, (g) cross sectional image of MMM containing 20 wt.% of NH2-MIL 53 with membrane thickness
263x284mm (96 x 96 DPI)

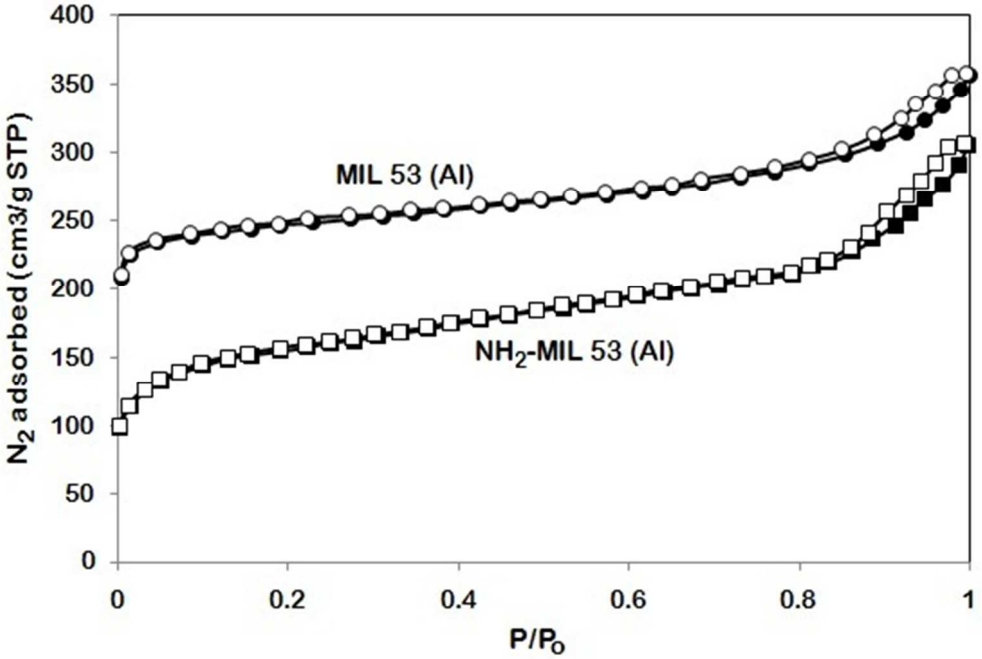

Fig. 8. N2 adsorption- desorption of MIL 53 and NH2-MIL 53 at 77 K
146x97mm (96 x 96 DPI)

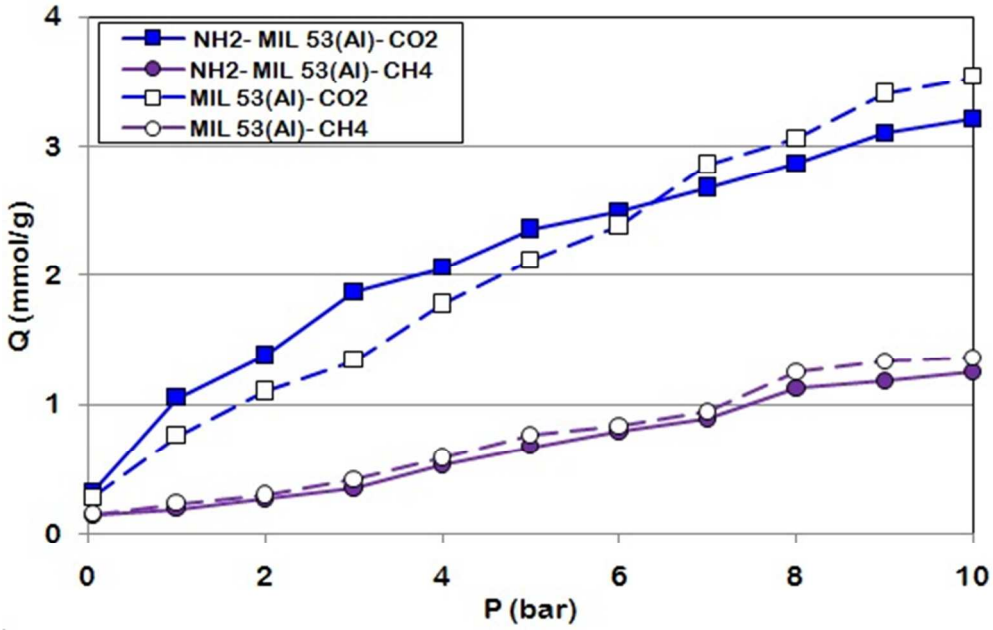

Fig. 9. CO2 and CH4 adsorption isotherms of MIL 53 and NH2-MIL 53 samples at 30 ºC
147x95mm (96 x 96 DPI)

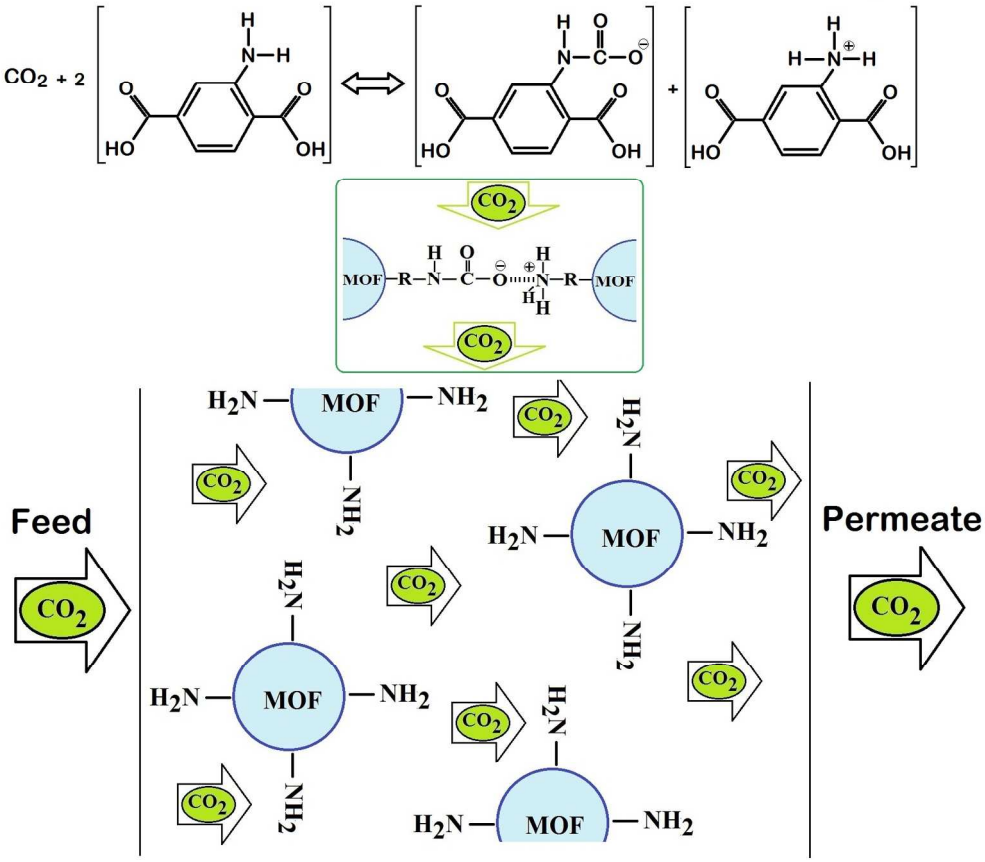

Fig. 10. Schematic view of reaction between CO2 and R-NH2 group to form carbomate formation where facilitated the CO2 permeation
498x434mm (96 x 96 DPI)

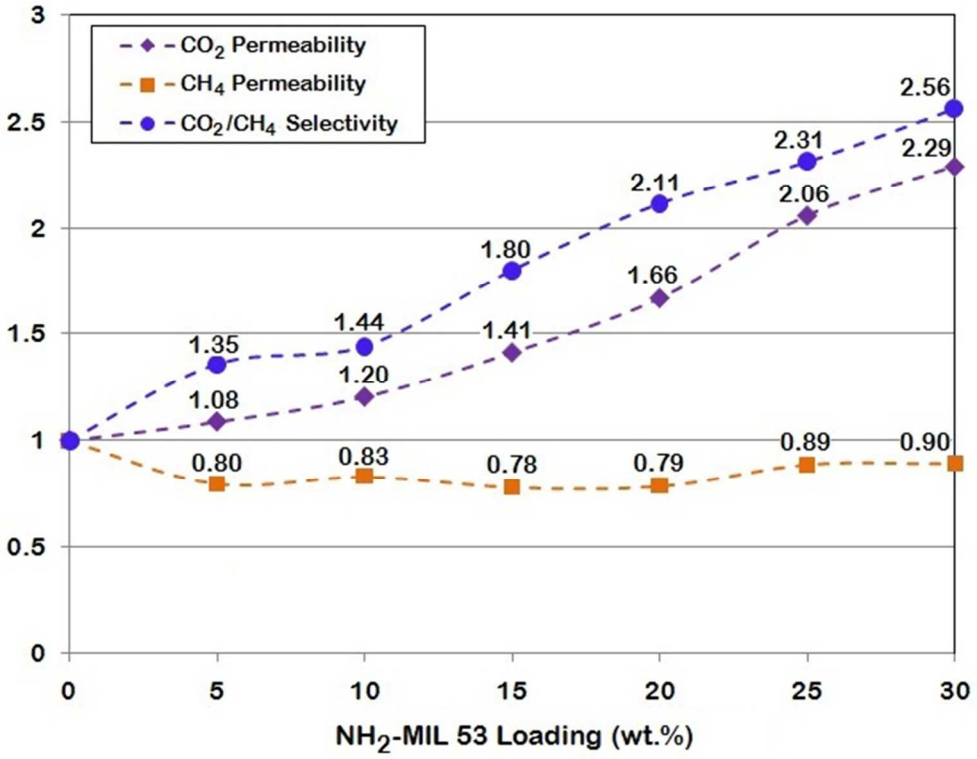

Fig. 11. Normalized permeabilities of CO2 and CH4 gases and CO2/CH4 ideal selectivities versus NH2-MIL 53 loading
166x129mm (96 x 96 DPI)

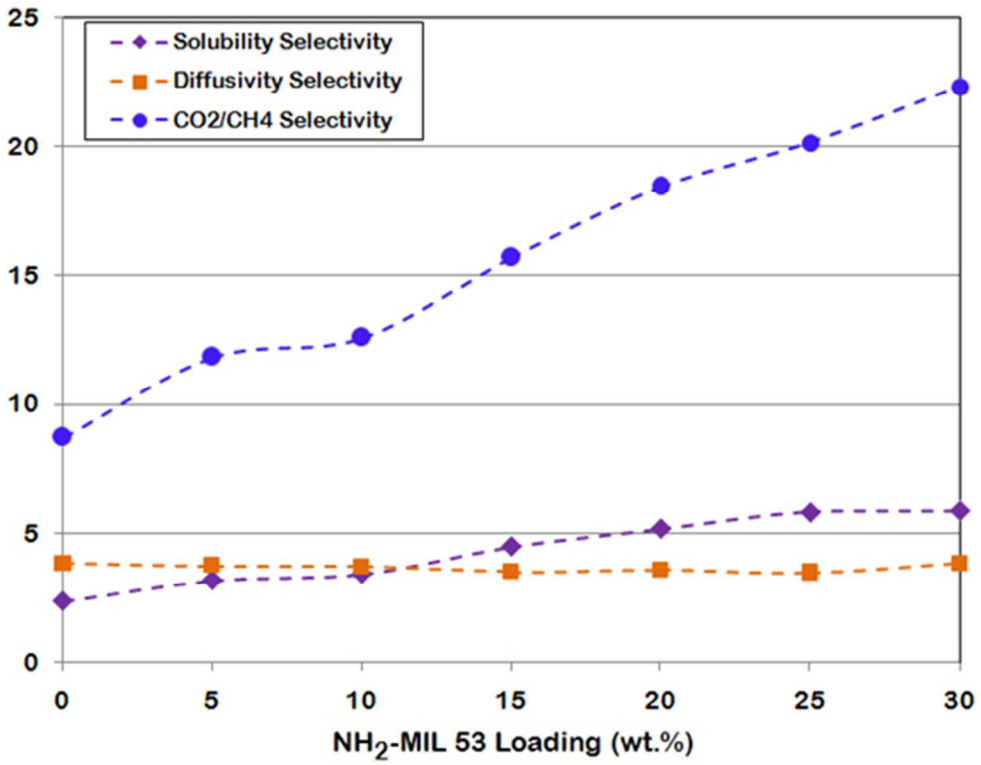

Fig. 12. Effect of NH2-MIL 53 loading on solubility, diffusivity and CO2/CH4 ideal selectivities
155x121mm (96 x 96 DPI)

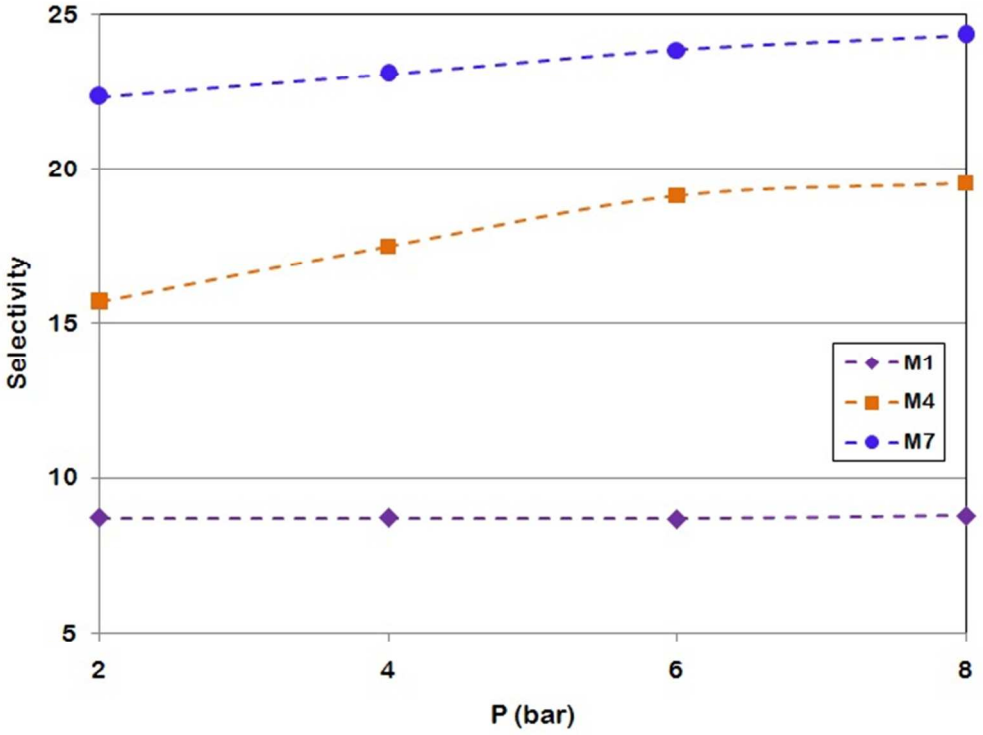

Fig. 13. Effect of pressure on the selectivity of neat PMP (M1) and MMMs (M4 and M7)
171x129mm (96 x 96 DPI)

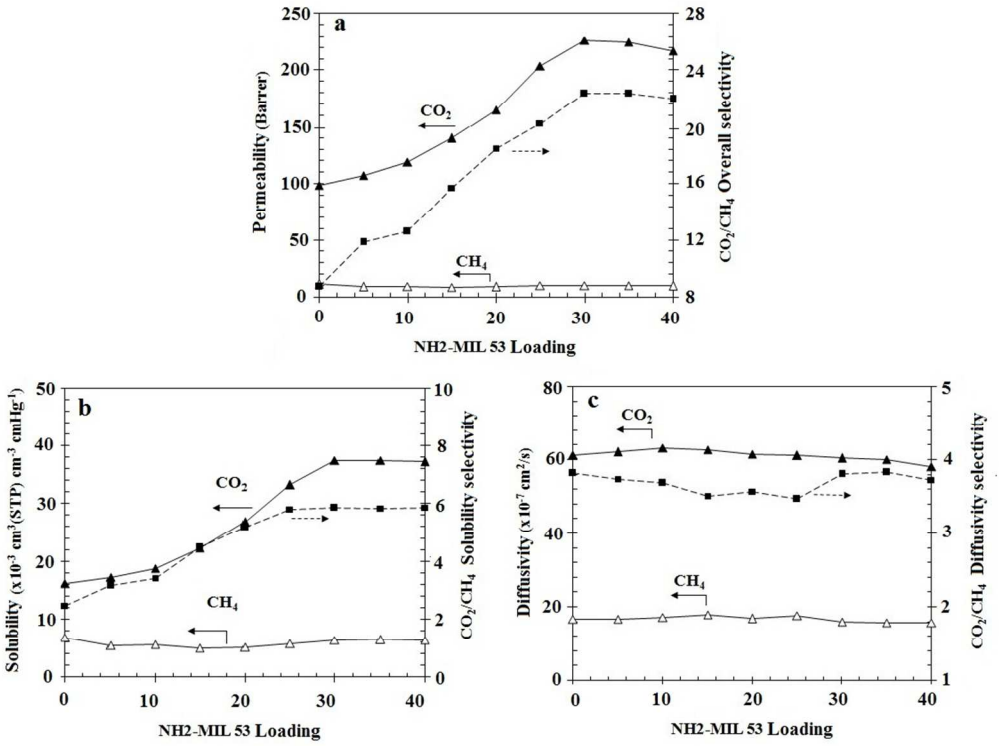

Fig. 14. The effect of NH2-MIL 53 loading on (a) permeability and CO2/CH4 selectivity, (b) solubility and CO2/CH4 solubility selectivity (c) diffusivity and CO2/CH4 diffusivity selectivity
297x223mm (96 x 96 DPI)

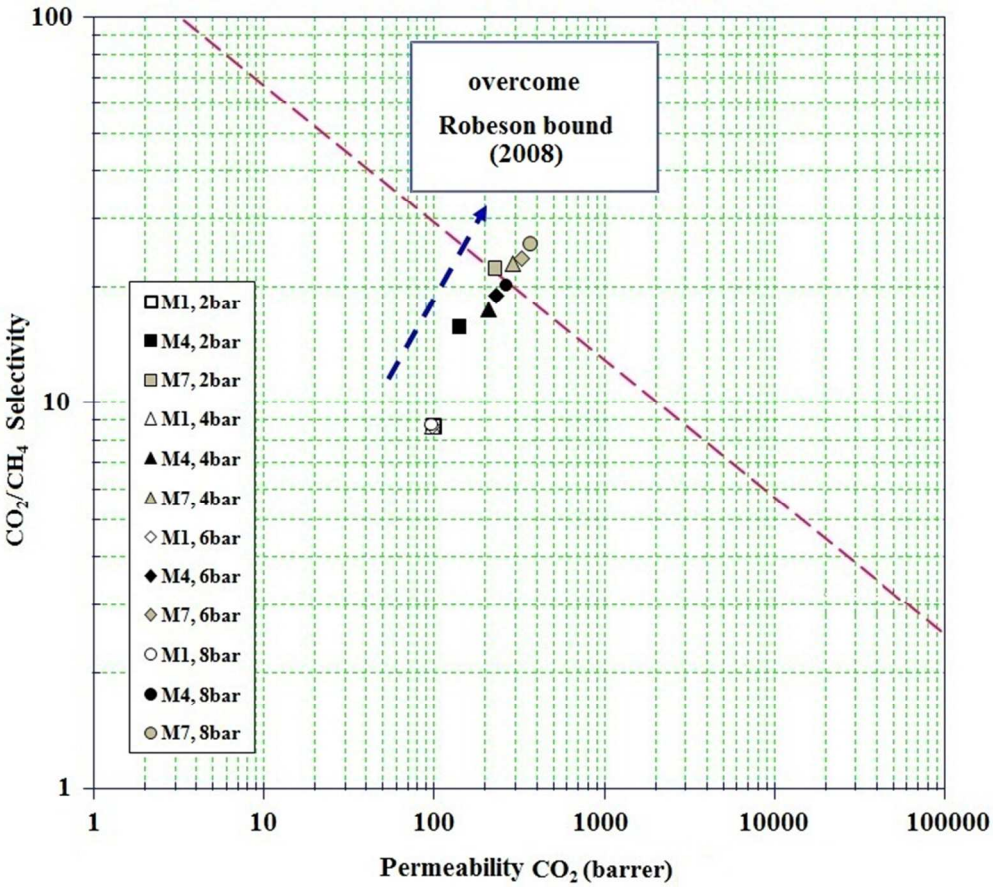

Fig. 15. Performance of synthesized MMMs prepared with different weight fractions of NH2-MIL 53 as well as pure PMP membrane in pure gas permeation compared to Robeson upper bound at 2, 4, 6 and 8 bar
207x187mm (96 x 96 DPI)

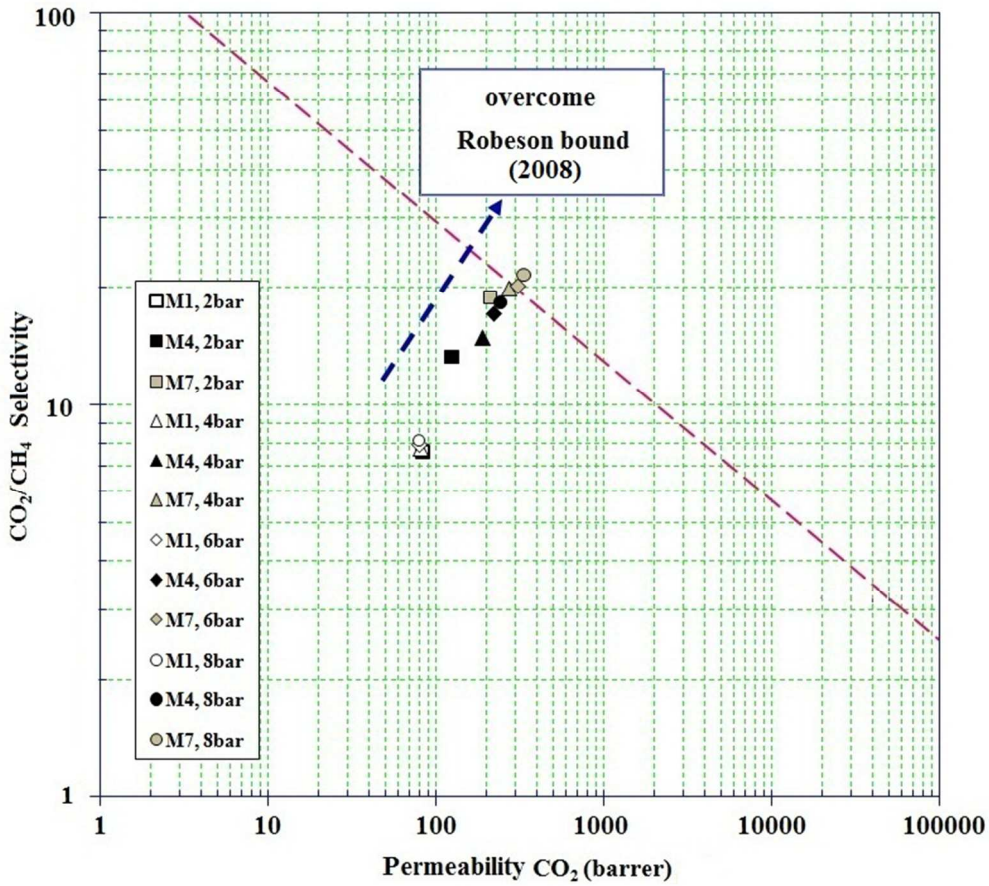

Fig. 16. Performance of synthesized MMMs prepared with different weight fractions of NH2-MIL 53 as well as pure PMP membrane in mixed gas permeation compared to Robeson upper bound at 2, 4, 6 and 8 bar
209x187mm (96 x 96 DPI)